Schweizerische Eidgenossenschaft
Confédération suisse
Confederazione Svizzera
Confederaziun svizra

Federal Department of the Environment, Transport, Energy and Communications DETEC

Swiss Federal Office of Energy SFOE
Energy Research and Cleantech Division

Final report dated 15-12-2023

AMSimLOCA - Advanced Modelling and Simulation of Nuclear Fuel Behaviour based on LOCA tests at the MIR reactor

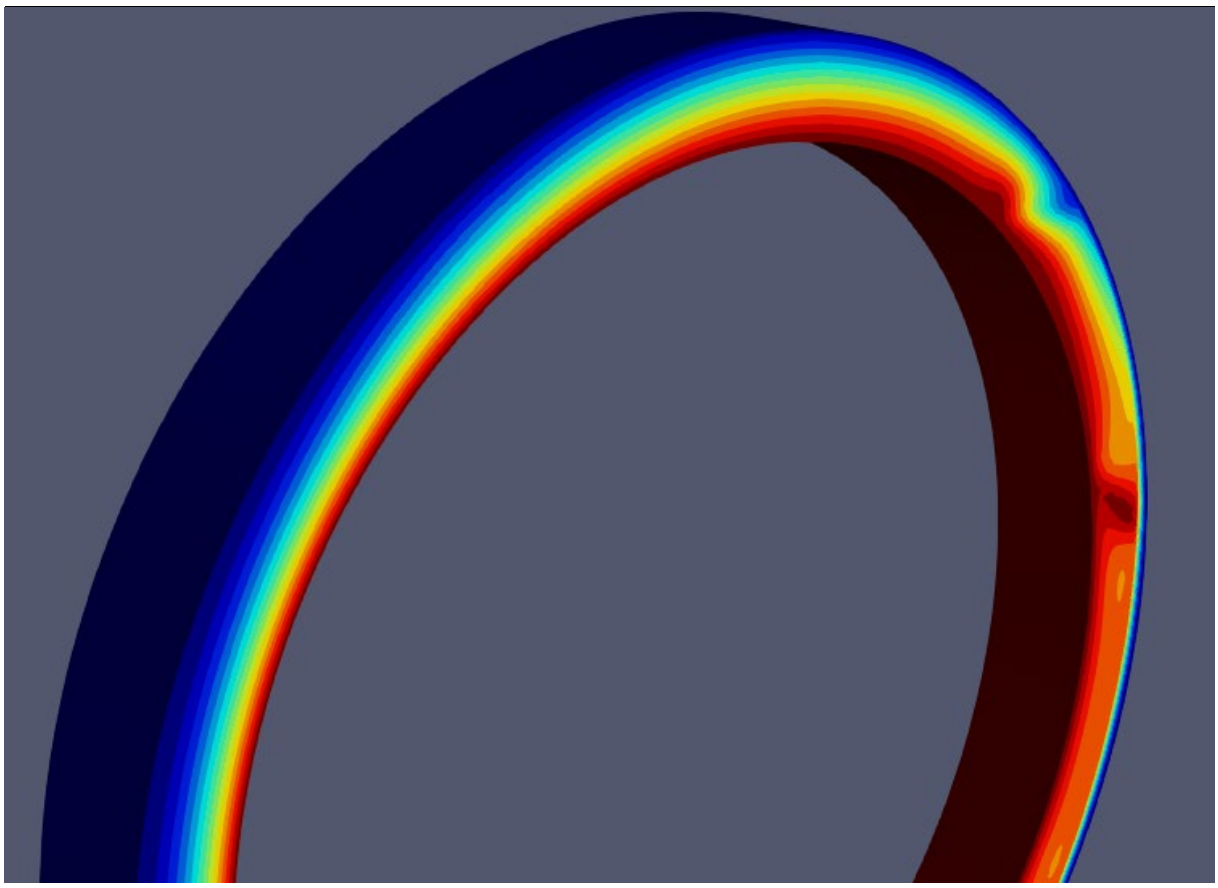

Source: EPFL, Laboratory for Reactor Physics and System Behavior, 2023

Date: 15-12-2023

Location: Bern

Publisher:
Swiss Federal Office of Energy SFOE
Energy Research and Cleantech
CH-3003 Bern
www.bfe.admin.ch

Subsidy recipients:
Ecole Polytechnique Fédérale de Lausanne (EPFL)
Laboratory for Reactor Physics and Systems Behaviour (SB IPHYS LRS)
Station 3, Bâtiment PH
CH-1015 Lausanne
www.epfl.ch

Authors:
Scolaro, Alessandro, EPFL, alessandro.scolaro@epfl.ch
Andreas, Pautz, EPFL, andreas.pautz@epfl.ch

SFOE project coordinator:
Michael Moser: michael.moser@bfe.admin.ch

SFOE contract number: SI/502311-01

Zusammenfassung

Das Projekt AMSimLOCA ist eng in eine langfristige wissenschaftliche Zusammenarbeit zwischen dem Labor für Reaktorphysik und Systemverhalten an der EPFL und dem Commissariat à l'Énergie Atomique et aux Énergies Alternatives (CEA, Frankreich) auf dem Gebiet der Sicherheit von Leichtwasserreaktoren (LWR) eingebettet. Es nimmt Kredit vom laufenden OECD/Nuclear Energy Agency (NEA) Framework for Irradiation Experiments (FIDES) und konzentriert sich auf die Modellierung und Simulation von LWR-Kernbrennstoffen unter Störfallbedingungen. Der anfängliche Schwerpunkt lag auf dem Brennstoffverhalten bei einem postulierten Kühlmittelverlustunfall (LOCA), mit Validierungsdaten, die vom MIR-Reaktor in Russland hätten geliefert werden sollen. Angesichts der aktuellen geopolitischen Lage und der Unmöglichkeit, Daten aus dem MIR-Reaktor zu erhalten, wurde gemeinsam mit der CEA beschlossen, den Schwerpunkt des Projekts durch die Beteiligung an einem weiteren FIDES-Projekt (HERA: High Burnup Experiments in Reactivity Initiated Accidents) auf Reaktivitätsstörfälle (RIAs) auszuweiten. HERA wird Validierungsdaten zur Verfügung stellen, die aus Messungen am TREAT-Reaktor der Idaho National Laboratories, USA, gewonnen werden. Die Aktivitäten konzentrierten sich daher auf die Erweiterung des EPFL-eigenen OFFBEAT-Brennstabverhalten-Codes für die Analyse von LWR-Störfallbedingungen. Dank dieser Entwicklungsarbeit kann OFFBEAT sowohl für die Analyse von LOCAs als auch von RIAs eingesetzt werden, und es wird an der Vorbereitung der Eingabedateien für die Simulation der Experimente gearbeitet, die im TREAT-Reaktor durchgeführt werden sollen.

Résumé

Le projet AMSimLOCA est étroitement lié à une collaboration scientifique à long terme entre le Laboratoire de physique des réacteurs et de comportement des systèmes de l'EPFL et le Commissariat à l'Énergie Atomique et aux Énergies Alternatives (CEA, France) dans le domaine de la sûreté des réacteurs à eau légère (REL). Il emprunte à l'actuel Framework for Irradiation Experiments (FIDES) de l'OCDE/Agence de l'énergie nucléaire (AEN) et se concentre sur la modélisation et la simulation du combustible nucléaire des REL dans des conditions accidentelles. L'accent initial a été mis sur le comportement du combustible en cas d'accident postulé de perte de réfrigérant (LOCA), avec des données de validation qui auraient dû être fournies par le réacteur MIR en Russie. Compte tenu de la situation géopolitique actuelle et de l'impossibilité d'obtenir des données du réacteur MIR, il a été décidé, en collaboration avec le CEA, d'élargir l'axe du projet aux accidents de réactivité (RIA) en participant à un autre projet FIDES (HERA : High Burnup Experiments in Reactivity Initiated Accidents). HERA fournira des données de validation obtenues à partir de mesures effectuées sur le réacteur TREAT des Idaho National Laboratories, aux États-Unis. Les activités se sont donc concentrées sur l'extension du code de comportement du crayon combustible OFFBEAT propre à l'EPFL pour l'analyse des conditions d'accident REL. Grâce à ce travail de développement, OFFBEAT peut être utilisé aussi bien pour l'analyse des LOCA que des RIA, et des travaux sont en cours pour préparer les fichiers d'entrée pour la simulation des expériences qui seront menées dans le réacteur TREAT.

Summary

The project AMSimLOCA is tightly integrated into a long-term scientific collaboration between the Laboratory for Reactor Physics and System Behaviour at the EPFL and the Commissariat à l'Énergie Atomique et aux Énergies Alternatives (CEA, France) in the field of Light Water Reactor (LWR) safety. It benefits from the ongoing OECD/NEA Framework for Irradiation Experiments (FIDES) and it focuses

on the modelling and simulation of LWR nuclear fuel. The initial focus was on fuel behavior during a postulated Loss of Coolant Accident (LOCA), with validation data that should have been provided by the MIR reactor in Russia. In view of the current geopolitical situation and the impossibility to receive data from the MIR reactor, it was decided, together with the CEA, to expand the focus of the project to Reactivity-Initiated Accidents (RIAs) via participation to another FIDES project named HERA (High Burnup Experiments in Reactivity Initiated Accident). HERA will provide validation data obtained in the TREAT reactor in the US. The activities have thus focused on the extension of the in-house OFFBEAT code for the analysis of accidental conditions. This development work allows OFFBEAT to be employed for the analysis of both LOCAs and RIAs, and work is ongoing to prepare the input decks for the simulation of the experiments that will be carried out in the TREAT reactor.

Contents

Abbreviations

CEA - Commissariat à l'Énergie Atomique et aux Énergies Alternatives

FIDES - Framework for Irradiation Experiments

HERA - High Burnup Experiments in Reactivity Initiated Accident

LOCA – Loss-Of-Coolant Accident

LWR – Light Water Reactor

RIA – Reactivity-Initiated Accident

JEEP - Joint Experimental Program (within the FIDES framework program)

1 Introduction

1.1 Background information and current situation

Both the École Polytechnique Fédérale de Lausanne (EPFL) and the French Commissariat à l'Énergie Atomique et aux Énergies Alternatives (CEA) have been continuously progressing on the development of advanced simulation software for the multi-dimensional, high-fidelity analysis of nuclear fuel behavior in the past years. In particular, the ALCYONE code is under development at the CEA, and the OFFBEAT code is developed at the EPFL. The need for advanced tools for the investigation of nuclear fuel behavior is corroborated by several international activities carried out in this research area. Besides ALCYONE and OFFBEAT, developments of advanced tools of this type are being pursued at the Idaho National Laboratory, USA (the BISON code) and at the Comisión Nacional de Energía Atómica, Argentina (the DIONISIO code). The objective of these developments is to investigate poorly-known non-symmetric scenarios in Light Water Reactor (LWR) fuel, as well as to improve our understanding of nuclear fuel via a more mechanistic description of its behavior, compared to legacy one-dimensional fuel behavior codes. In Switzerland, the interest in multi-dimensional fuel behavior was triggered by a fuel failure at the Leibstadt power plant that caused a prolonged shutdown with significant economic repercussions, and that highlighted the lack of readily available tools for complex multi-dimensional and multi-physics investigations. Development of these advanced simulation tools requires extensive verification and validation. Unfortunately, limited data are publicly available for code validation, while code verification activities against other codes are made difficult by the limited number of advanced multi-dimensional fuel behavior tools and, often, by their proprietary nature. The AMSimLOCA attempts to address some of these knowledge gaps by providing open access to state-of-the-art simulation software, in particular OFFBEAT, combined with access to some of the most recent experimental data available.

The work performed during the first year (2022) of the AMSimLOCA project was dedicated to the extension of the OFFBEAT code for the analysis of accidental transients in LWRs. In particular, OFFBEAT was extended towards the simulation of finite strains, which allows for improved predictions in accidental scenarios involving large deformation of the cladding. In addition, high-temperature models have been included for creep, Zircaloy phase-transition and cladding burst. A code validation has been performed against the well-known PUZRY and the IFA-650.2 LOCA experiments (see Appendix A). For both cases, the validation has demonstrated good predictive capabilities of the OFFBEAT fuel performance code, showing good agreement with experimental data, and a response that is consistent with the predictions of other fuel performance codes where similar models and capabilities had already been implemented previously. The discrepancies observed with respect to the experimental measurements can be associated with the unavailability of several key parameters for the simulated rods, such as an accurate temperature profile on the outer surface of the cladding. Other possible reasons have been identified, e.g. the absence of models accounting for the mechanical anisotropy of α-phase Zircaloy, or the uncertainties of the high-temperature creep model in the temperature range characterized by the coexistence of α- and β-Zirconium phases. Details of the work that has been performed within this project can be found in Appendix A, which contains a 2023 publication in the renowned journal “Nuclear Engineering and Design”. The project work has also been previously reported in the 2022 project interim report to AMSimLOCA.

This final report aims to summarize the developments and simulations performed with the OFFBEAT code, particularly during the second year of the AMSimLOCA project and thus addressing the most recent highlights. The collaboration with the CEA through a postdoctoral researcher jointly hired by EPFL and CEA was well integrated therein. Furthermore, the project benefits enormously from the ongoing Framework for IrraDiation Experiments (FIDES) under the auspices of the OECD/NEA, of which Switzerland is a partner through the membership of the Paul Scherrer Institut (PSI), the Federal Nuclear Safety Inspectorate ENSI, and EPFL itself.

As mentioned above, the initial aim of the AMSimLOCA project was to model LWR (Light Water Reactor) nuclear fuel rods during hypothetical Loss of Coolant Accidents (LOCA) scenarios. The original plan

involved simulations with both OFFBEAT and the CEA code ALCYONE, specifically for LOCA tests conducted at the MIR reactor in Russia using VVER-type fuel. However, due to the unforeseen challenges represented by the geopolitical crisis emerging from the armed conflict between Russia and Ukraine, this original plan was deemed not feasible anymore by both EPFL and CEA. Consequently, the project's focus shifted from LOCA to Reactivity-Initiated Accident (RIA) analysis - a choice that was made possible thanks to the Joint Experimental Program (JEEP) known as High-burnup Experiments for Reactivity Initiated Accident (HERA), which is, like the originally intended MIR experiments, also part of the OECD/NEA FIDES framework. Despite this change in focus, the core objectives of the project remain valid and the same: to validate, calibrate, and advance the development of the two fuel performance codes OFFBEAT and ALCYONE for accidental analysis using recent experimental data. Additionally, the aim is to perform a pioneering code-to-code benchmark focused on two modern multidimensional tools such as ALCYONE and OFFBEAT.

The final year's initial months were spent to train the jointly hired CEA-EPFL postdoctoral researcher appropriately, and getting him acquainted with OFFBEAT, as well as implementing the necessary physical models for the simulation of the 12 RIA pulses conducted during 2023, both in the TREAT (USA) and NSRR (Japan) research reactors on unirradiated fuel rods consisting of UO_2-Zy4. In what follows, these 12 test pulses will be referred to as the Phase 1 of the HERA project. The results of these simulations were presented and discussed during an international HERA project meeting bringing together 23 organisations and 15 fuel performance codes. The goal of the exercise was to predict the failure or non-failure of the fuel rods by pellet-clad mechanical interaction (PCMI) during the pulses. Once the simulations related to the first phase of the HERA project were finished, new developments efforts were undertaken. Two main axes of developments, aiming to propose a complete RIA simulation tool for irradiated fuel rods were identified:

1. The implementation, verification, and validation of a hydrogen model. This model should be able to simulate the hydrogen intake during base irradiation, the hydrogen diffusion into the clad due to a concentration or temperature gradient and, finally, the precipitation of hydrogen into solid hydrides. Solid hydrides are a factor of embrittlement of the clad facilitating its rupture by PCMI. Consequently, the knowledge of the hydrogen local concentrations is of importance for the accurate prediction of clad failure during an accidental transient such as a RIA.

2. The implementation, verification, and validation of a damage model to simulate the UO_2 mechanical behaviour, specifically its fragmentation due to high compressive stresses. This damage model aims to simulate the fragmentation of the fuel that can be observed during a RIA transient and was previously developed and used during the PhD thesis of M. Reymond [1]. The fragmentation of the fuel matrix can lead to fission gas release and to an increase of the rod internal pressure. The accurate simulation of the released quantity of gases and its kinetics is therefore also of importance for the prediction of clad failure during a RIA transient [2].

1.2 Purpose of the project

The main goal of this work is the validation, calibration and further development of the two fuel behavior codes developed by the EPFL and the CEA, based on new experimental data on Reactivity Initiated Accident (RIA) conditions from the HERA JEEP. In addition, the concurrent availability in the project of two modern multi-dimensional codes for fuel behavior will be employed to allow for a first-of-a-kind detailed code-to-code benchmark. This will improve the modelling predictions of our codes and provide additional credibility about their applicability to problems of practical interest.

1.3 Objectives

The project will help validate and calibrate the OFFBEAT simulation and modelling tool for the analysis of nuclear fuel. The tool is planned for application to the analysis of the nuclear fuel in power plants, thus contributing to the safe and reliable operation of nuclear power plants in Switzerland.

The project also fits into an important collaboration between the LRS at the EPFL and the Commissariat à l'Energie Atomique (CEA, France) in the OECD/NEA Framework for Irradiation Experiments (FIDES).

In addition, the project will contribute to the EPFL activities as an International Atomic Energy Agency (IAEA) Collaborating Center, which has been recently (as of September 26, 2023) re-designated in the field of open-source tools and open-access data in nuclear simulation.

2 Simulations of Phase 1 of the HERA JEEP

The 12 simulated test pulses of the phase 1 of the HERA JEEP project have the following characteristics:

- Full-width half maximum of the power pulse ranging from 7.5 to 300 ms.
- Deposited energy during pulse ranging from 600 to 850 J/g.
- Pre-hydrided Zy-4 cladding with a concentration of hydrogen ranging from 400 to 1200 wt.ppm and an external rim thickness ranging from 40 to 140 µm.
- Oversized fuel pellet made of unirradiated UO_2 to simulate the partial closing of the pellet-clad gap.

2D axisymmetric fuel rod models were created for this exercise, with the governing equations solved along the r- and z-directions. The fuel pellets were treated as a smeared column that deforms by thermo-elasticity, while fuel creep, fuel cracking, relocation and densification models were not activated – a good approximation for unirradiated pellets.

In order to accurately simulate the mechanical behaviour of the cladding and its stress state, the elasto-viscoplastic model of Le Saux et al [3] also known as the GPLS, by the name of its authors, was implemented in OFFBEAT. As this mechanical law considers the cladding orthotropic nature, its implementation in OFFBEAT required development of a framework – at the time missing - for the manipulation of a 4th order tensor. The newly implemented GPLS law was verified on simplified test cases, by simulating the deformation of a single cell as a function of number of parameters (strain rate, loading path, temperature etc). The results were compared to verification tests made available by the CEA using their in-house MFront code (Figure 1). Wherever possible, results were also verified against the analytical solution.

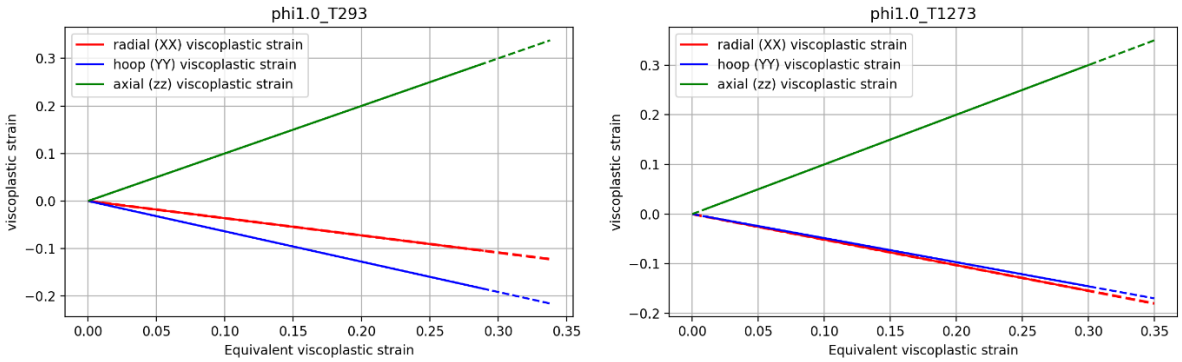

Figure 1: Comparison between OFFBEAT (lines) and MFront (dashed lines) simulations of uniaxial traction tests on Zy-4 with the GPLS. Fast neutron (E > 1MeV) fluence of $10x10^{25}$ nm^{-2} and temperature of 293 (left) and 1273 (right) K.

Additionally, in order to accurately assess the cladding failure during a RIA transient, the failure criterion of Jernkvist et al [4] was added to OFFBEAT. This criterion considers the temperature, strain rate and the average hydrogen content of the cladding but does not depend on the rim thickness. A modification of the failure criterion introducing a dependency on the rim thickness has been proposed by J. Sercombe and used in the ALCYONE 1.5D simulations of the phase 1 of the HERA benchmark. Its usage in OFFBEAT is envisioned for future code versions.

For the outer thermal boundary conditions, as OFFBEAT does not have a dedicated thermo-hydraulic sub-solver or coolant channel model, the cladding external temperature was imposed either based on RELAP calculations made available by the Idaho National Laboratories for the benchmark participants, or based on ALCYONE calculations made available by CEA Cadarache.

During these first months of 2023, discussions were routinely held with the researchers of CEA Cadarache and the developments were also validated sequentially by performing code-to-code comparisons with the results of the simulations obtained by the CEA Cadarache, using their 1.5D scheme of the ALCYONE RIA fuel performance code.

Thanks to the developments described above, the final OFFBEAT results for phase 1 proved to be in line with those obtained with the ALCYONE fuel code (which uses the same cladding mechanical behavioural law). More generally, we also found reasonable agreement with the majority of the results presented during the international meeting concluding the Modelisation & Simulation (M&S) exercise of the phase 1 of the HERA Project. Some relevant discrepancies between different codes (and sometimes even between different institutions using the same code) were however outlined, as one can see for the clad failure prediction output (a value of 1 indicating a failure of the clad) plotted as a function of time for the HERA5 pulse on Figure 2.

These findings indicate that OFFBEAT has been brought to maturity in a relatively short period of time regarding the simulation of RIA transient scenarios, at least for what concerns unirradiated fuel rods. Indeed, while an important scatter exists between the codes and organisations, OFFBEAT's results were consistently in line with the average of benchmark participants' solutions.

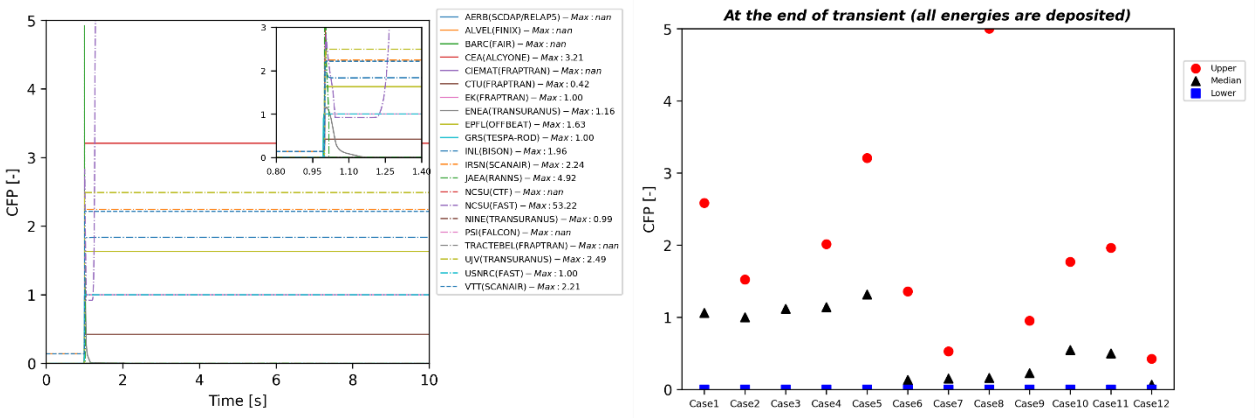

Figure 2: Clad Failure Prediction (CFP) criterion calculated by the participants of the M&S exercise of the phase 1 of the HERA project. Left: as a function of time for the HERA5 test pulse (NSRR, 7.5ms FWMH, 750 j/g) and at the end of the transients for all cases (right). A value egal or greater than 1 indicates that the clad is considered as failed according to the used criterion.

Nevertheless, it needs to be stressed that to date, the experimental data relative to the considered 12 pulses have not yet been made available and it is not possible to propose a code-to-experimental data comparison. Also, the simulation of the clad-to-coolant heat exchange is one of the main difficulties when it comes to RIA simulations, and this capability is still lacking from OFFBEAT. Efforts are currently underway at EPFL to enable the coupling between OFFBEAT and the GeN-Foam multiphysics platform [5], also developed at EPFL and throughout based on the OpenFOAM library.

3 Developments to Enable the Analysis of Irradiated Fuel Rods

The next step of the AMSimLOCA project in 2023 was to focus on the developments and implementation of physical models for the simulation of RIA transients on irradiated fuel rods. As previously stated, two

main differences between irradiated and unirradiated fuel rods can be outlined in the context of the study of cladding failure during a RIA:

1. The cladding wall presents a hydrogen profile due to hydrogen pick-up and migration during base irradiation. Additionally, if spalling of the outer zirconia layer occurs, the resulting local cold spot triggers hydrogen migration and the formation of a so-called hydride blister. These hydride blisters significantly decrease the cladding mechanical resistance and are a preferential site for cladding failure to occur during the PCMI phase of a RIA transient. In Zircaloy-4 cladding, the typical geometry of a blister is around 1-5 mm in diameter and about half of the thickness of the tube [6].

2. The irradiated fuel has a considerable inventory of fission gases stored in the grain or at the grain boundaries. Other notable changes include cracking of the pellets and the formation of the so-called rim microstructure at the periphery of the pellets in the case of high burn-up fuel. A realistic simulation of a RIA transient conducted on irradiated fuel rod must thus include a model able to simulate the fission gas release and the subsequent increase of internal pressure.

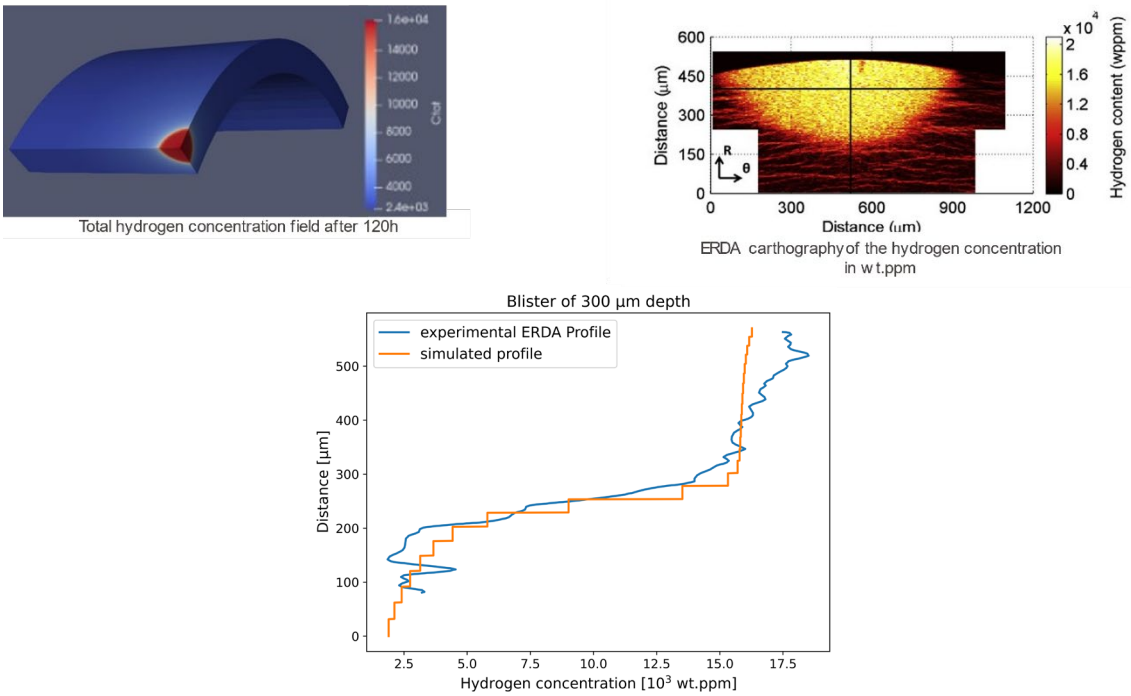

Figure 3: Hydride blister in the experiment of Helouin de Menibus (top right) and numerical result obtained with OFFBEAT (top left). On the bottom, the hydrogen concentration obtained with OFFBEAT along the depth of the blister is well reproduced.

Regarding hydrogen migration, the final goal is to be able to accurately predict the hydrogen distribution in the cladding before the transient. It would then be possible to use or to develop mechanical behavioural laws, depending on the local concentration of hydrogen and rim thickness. For example, the GPLS already implemented in OFFBEAT was also expressed as a function of the local concentration of hydrogen in solid solution and in solid precipitate in the PhD thesis of M. Le Saux [7]. Consequently, efforts were carried out to implement hydrogen transport models (i.e. diffusion equation-based) and hydrides precipitation models in OFFBEAT.

Two models for the hydrides precipitation and dissolution were introduced, i.e. the Hydride Nucleation-Growth-Dissolution (HNGD) already present in BISON and the Johnson-Mehl-Avrami-Kolmogorov model [6], [8]–[10]. Validation of these two models is still currently ongoing, based on available data in

the literature [6], [11]–[14], but encouraging results were already obtained. In particular, OFFBEAT was used to reproduce the experiment of Arthur Helouin de Menibus [19], where the growth of a hydride blister by thermo-diffusion was obtained by applying a cold spot to a hydrogen-charged tubular sample. As shown in Figure 3 above, the shape of the blister and its depth are well captured with OFFBEAT.

Regarding the fission gas release and damage during the transient, the approach chosen in this project is based on the μ-model [17] already employed during the PhD thesis of M. Reymond [1]. This model describes the loss of stiffness of the material by calculating a scalar damage quantity, D, ranging from 0 to 1, which is used to progressively decrease the elastic modulus of the material. A damage value of 1 indicates a complete loss of integrity of the material and it translates into an elastic modulus close to 0. This μ-model has been implemented in OFFBEAT and validated against MTest simulations on a material point.

The fission gas behavior is included in OFFBEAT via SCIANTIX [18], a 0-D open-source code developed at Politecnico di Milano. The models implemented in SCIANTIX cover both the intra-granular and inter-granular inert gas behavior. SCIANTIX is wrapped in a C++ class within OFFBEAT to move data between the local scope (grain) of SCIANTIX and the larger scope (rod) of OFFBEAT. In the framework of this project, this OFFBEAT SCIANTIX-wrapping class has been modified to pass to SCIANTIX the value of damage calculated by the μ-model. In return, this damage variable is used during a RIA simulation to trigger the fission gas inventory of a given cell, once a threshold value is reached.

The well-known REP-Na4 (FWHM ~75 ms) and REP-Na5 (FWHM ~9 ms) test cases were used as preliminary validation for the fragmentation and release models. Indeed, CEA made available some sanitized but representative data sets for the base irradiation of the father rod, as well as for the subsequent RIA-like pulses. These two experiments are of interest since the two rodlets were fabricated from the same father rod but led to a different amount of release (8% and 15% for REP-Na4 and 5, respectively) for a similar total energy deposition [15]. It is thought that the difference in kinetic of the pulses (much shorter on REP-Na5), caused a different mechanical loading and fragmentation pattern (significantly larger on REP-Na5), leading to a notable difference in release fraction.

The results of this first exercise are very promising, at least qualitatively. Indeed, as shown in Figure 4 below, OFFBEAT is able to replicate the difference in the extent of the damaged zone between REP-Na5 (almost a third of the rod from the outer rim) and REP-Na4 (a small fraction of damage). The slight overestimation of damage in REP-Na4 – no fragmentation was detected experimentally - might result from the fact that peak power level data (linear heat rate and cladding outer temperature) were applied axially to the entire rod for this preliminary analysis. Similarly, the simulations are also able to replicate the difference in release ratio between the two rods, although the actual final value is very sensible on the damage threshold selected for considering a complete release of the gases from the grains.

4 Conclusions and Outlook

To conclude, the open-source fuel performance code OFFBEAT was enhanced to enable the simulation of RIA transients for unirradiated fuel rods. This necessitated the implementation of relevant physical models and their verification. The results obtained from data of the first phase of the HERA JEEP are promising, as they are in agreement with those obtained using more mature codes. In the future, if provided, comparison with experimental data will be of particular interest.

OFFBEAT is now being enabled to perform RIA analysis on irradiated rods. To this end, developments efforts were dedicated during this project to the implementation of hydrogen pickup models, including its diffusion and its precipitation into solid hydrides. The hydrogen distribution calculated by OFFBEAT was verified for simplified cases and it was validated against an asymmetric experiment showing a localized blister, reproducing with accuracy the shape of the blister as well as the hydrogen concentration along its depth.

Finally, a mechanistic model for fuel fragmentation due to high compressive stresses was implemented to predict the extent of the damaged zone in the pellet and drive the fission gas release during a fast transient such as RIA. The simulation of the REP-Na4 and REP-Na5 test pulses showed the feasibility of the proposed approach, and it will be presented at the SMiRT27 conference, which will be held in Japan in March 2024. The corresponding publication is attached to this report in Appendix B.

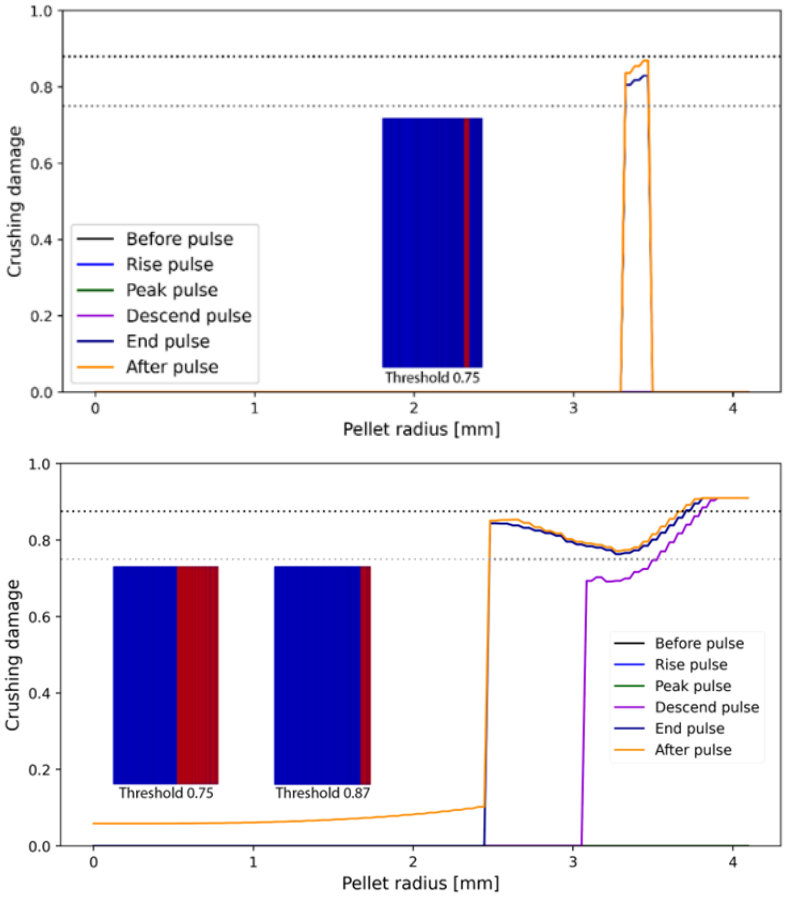

Figure 4: Damage zones for REP-Na4 (top) and REP-Na5 (bottom). OFFBEAT with the mu-model is able to reproduce the large fragmented zone seen experimentally for REP-Na5. The graphs include also a figure of the pellet with in red the cells where release due to fragmentation is considered. As it can be seen, the extent of this zone is very sensitive on the selected threshold to consider the full release from the grain.

5 National and international cooperation

The project is tightly integrated into a long-term scientific collaboration between the LRS at EPFL and the Commissariat à l'Énergie Atomique et aux Énergies Alternatives (CEA, France) in the field of LWR safety. It also benefits from the ongoing OECD/NEA Framework for Irradiation Experiments contributes to the EPFL activities as IAEA Collaborating Center in the field of open-source tools and open-access data in the nuclear field

6 Publications Resulting from this Project

Appendix A: E. Brunetto et al., “Extension of the OFFBEAT Fuel Performance Code to Finite Strains and Validation Against LOCA Experiments”. Published in *Nuclear Engineering and Design* 406 (2023), https://doi.org/10.1016/j.nucengdes.2023.112232

Appendix B: M. Reymond et al., “A damage model to describe fuel fragmentation and predict fission gas release during Reactivity Initiated Accident”, submitted to the “27th International Conference on Structural Mechanics in Reactor Technology” (SMIRT27), Yokohama, March 3-8, 2024

7 References

[1] M. Reymond, J. Sercombe, L. Gallais, T. Doualle, and Y. Pontillon, “Thermo-mechanical simulations of laser heating experiments on UO2,” Journal of Nuclear Materials, vol. 557, Dec. 2021, doi: 10.1016/J.JNUCMAT.2021.153220.

[2] I. Guénot-Delahaie, J. Sercombe, É. Fédérici, C. Bernaudat, R. Largenton, and X. Haller, “Investigation of clad ballooning during NSRR RIA tests using ALCYONE fuel performance code,” Journal of Nuclear Materials, vol. 562, Apr. 2022, doi: 10.1016/j.jnucmat.2022.153584.

[3] M. Le Saux, J. Besson, S. Carassou, C. Poussard, and X. Averty, “A model to describe the anisotropic viscoplastic mechanical behavior of fresh and irradiated Zircaloy-4 fuel claddings under RIA loading conditions,” Journal of Nuclear Materials, vol. 378, no. 1, pp. 60–69, Aug. 2008, doi: 10.1016/J.JNUCMAT.2008.04.017.

[4] L. O. Jernkvist, A. R. Massih, and P. Rudling, “A Strain-based Clad Failure Criterion for Reactivity Initiated Accidents in Light Water Reactors SKI Perspective Background and purpose of the project,” 2004.

[5] C. Fiorina, I. Clifford, M. Aufiero, and K. Mikityuk, “GeN-Foam: a novel OpenFOAM® based multi-physics solver for 2D/3D transient analysis of nuclear reactors,” Nuclear Engineering and Design, vol. 294, pp. 24–37, Dec. 2015, doi: 10.1016/J.NUCENGDES.2015.05.035.

[6] A. Hellouin De Menibus et al., “Formation and characterization of hydride blisters in Zircaloy-4 cladding tubes,” Journal of Nuclear Materials, vol. 449, no. 1–3, pp. 132–147, 2014, doi: 10.1016/j.jnucmat.2014.03.006.

[7] M. Le Saux, “Comportement et rupture de gaines en Zircaloy-4 détendu vierges, hydrurées ou irradiées en situation accidentelle de type RIA,” http://www.theses.fr, Jan. 2008, Accessed: Jul. 03, 2023. [Online]. Available: http://www.theses.fr/2008ENMP1608

[8] F. Passelaigue, E. Lacroix, G. Pastore, and A. T. Motta, “Implementation and Validation of the Hydride Nucleation-Growth-Dissolution (HNGD) model in BISON,” Journal of Nuclear Materials, vol. 544, p. 152683, Feb. 2021, doi: 10.1016/J.JNUCMAT.2020.152683.

[9] F. Passelaigue, P. C. A. Simon, and A. T. Motta, “Predicting the hydride rim by improving the solubility limits in the Hydride Nucleation-Growth-Dissolution (HNGD) model.,” Journal of Nuclear Materials, vol. 558, Jan. 2022, doi: 10.1016/j.jnucmat.2021.153363.

[10] G. P. Marino, “Hydrogen supercharging in Zircaloy,” Materials Science and Engineering, vol. 7, no. 6, pp. 335–341, 1971, doi: 10.1016/0025-5416(71)90016-4.

[11] B. F. Kammenzind, D. G. Franklin, W. J. Duffin, and H. R. Peters, “Hydrogen pickup and redistribution in alpha-annealed Zircaloy-4,” Jun. 1996, doi: 10.2172/244661.

[12] A. Sawatzky, “Hydrogen in zircaloy-2: Its distribution and heat of transport,” Journal of Nuclear Materials, vol. 2, no. 4, pp. 321–328, 1960, doi: 10.1016/0022-3115(60)90004-0.

[13] O. Courty, A. T. Motta, and J. D. Hales, “Modeling and simulation of hydrogen behavior in Zircaloy-4 fuel cladding,” Journal of Nuclear Materials, vol. 452, no. 1–3, pp. 311–320, 2014, doi: 10.1016/j.jnucmat.2014.05.013.

[14] D. S. Stafford, “Multidimensional simulations of hydrides during fuel rod lifecycle,” Journal of Nuclear Materials, vol. 466, pp. 362–372, Nov. 2015, doi: 10.1016/j.jnucmat.2015.06.037.
[15] J. Papin et al., “Summary and interpretation of the CABRI REP-Na program,” Nucl Technol, vol. 157, no. 3, pp. 230–250, 2007, doi: 10.13182/NT07-A3815.
[16] J. Sercombe et al., “2D simulation of hydride blister cracking during a RIA transient with the fuel code ALCYONE,” EPJ Nuclear Sciences & Technologies, vol. 2, p. 22, 2016, doi: 10.1051/EPJN/2016016.
[17] J. Mazars, F. Hamon, and S. Grange, “A new 3D damage model for concrete under monotonic, cyclic and dynamic loadings,” Materials and Structures/Materiaux et Constructions, vol. 48, no. 11, pp. 3779–3793, Nov. 2015, doi: 10.1617/S11527-014-0439-8/FIGURES/13.
[18] D. Pizzocri, T. Barani, and L. Luzzi, “SCIANTIX: A new open source multi-scale code for fission gas behaviour modelling designed for nuclear fuel performance codes,” Journal of Nuclear Materials, vol. 532, p. 152042, Apr. 2020, doi: 10.1016/J.JNUCMAT.2020.152042.
[19] Arthur Hellouin de Menibus et al, Formation and characterization of hydride blisters in Zircaloy-4 cladding tubes, Journal of Nuclear Materials, vol. 449, 2014

Appendix A: “Extension of the OFFBEAT fuel performance code to finite strains and validation against LOCA experiments”

Nuclear Engineering and Design 406 (2023) 112232

Contents lists available at ScienceDirect

Nuclear Engineering and Design

journal homepage: www.elsevier.com/locate/nucengdes

Extension of the OFFBEAT fuel performance code to finite strains and validation against LOCA experiments

Edoardo Luciano Brunetto [a,*], Alessandro Scolaro [a], Carlo Fiorina [b], Andreas Pautz [a,c]

[a] École Polytechnique Fédérale de Lausanne (EPFL), Laboratory for Reactor Physics and System Behaviour, 1015 Lausanne, Switzerland
[b] Texas A&M University, Department of Nuclear Engineering, 423 Spence St, College Station, TX 77843, USA
[c] Paul Scherrer Institut (PSI), Nuclear Energy and Safety Department, 5232 Villigen, Switzerland

A B S T R A C T

The mechanical analysis of nuclear fuel behavior under base-irradiation conditions has traditionally been performed adopting the small-strain approximation. However, many cases of interest for fuel behavior involve the occurrence of large rod deformations that overcome the validity limits of the small-strain approach such as the cladding ballooning during Loss Of Coolant Accidents, the Pellet-Cladding Mechanical Interaction in case of a Missing Pellet Surface or bending experiments on spent fuel rods. For this reason, the mechanical framework of the open-source fuel performance code OFFBEAT is extended to finite strains. To allow for validation against cladding burst experiments, high-temperature models tailored for LOCA regime including creep, Zircaloy phase-transition and cladding burst criteria are also implemented in the code and described in the present work. The paper presents the implementation and the verification of the large-strain mechanical solver implemented in OFFBEAT, together with the results of the validation performed against the PUZRY and the IFA-650.2 LOCA experiments.

1. Introduction

During base irradiation the deformations occurring in a nuclear fuel rod are typically much smaller than its characteristic dimensions. In fact, for the study of nominal operating conditions, fuel performance codes typically perform the mechanical analysis by using the so-called small-strain approach, which simplifies the mathematical formulation of the governing equations by neglecting non-linear terms in the constitutive laws.

However, some scenarios of interest in the field of fuel behavior do not fall within the small-strain approximation domain, as they are characterized by large deformations or rotations. Some examples include the bowing of fuel assemblies in a PWR core (Wanninger et al., 2018), the cladding deformation in the presence of missing pellet surface defects (Spencer et al., 2016), the failure of aspherical TRISO particles (Jiang et al., 2022) or the bending experiments performed on spent fuel rods to assess their structural integrity (Vlassopoulos et al., 2018). Most notably large deformations become relevant for some postulated Design Basis Accidents (DBA) conditions such as Loss Of Coolant Accidents (LOCA).

The **O**pen**F**OAM **F**uel **BE**havior **A**nalysis **T**ool (OFFBEAT) is a multi-dimensional fuel performance code developed since 2017 at the Laboratory for Reactor Physics and System Behavior (LRS) of the École Polytechnique Fédérale de Lausanne (EPFL) in collaboration with the Paul Scherrer Institut (PSI). OFFBEAT solves the heat equation and the mechanical equilibrium in the fuel rod and it is provided with open-literature correlations for material properties mainly from MATPRO (Idaho National Engineering Laboratory, 1979). Behavioral models for fuel (relocation, densification and swelling) and cladding (irradiation growth) are included in the code together with plasticity and creep laws to capture the non-elastic deformations of the rod. A gap plenum model derived from FRAPCON (Geelhood et al., 2015) is used in the code to track the evolution of gap volume and composition. The open-source multi-scale code SCIANTIX (Pizzocri et al., 2020) is embedded in OFFBEAT to monitor the fission gas behavior. More details about the OFFBEAT code can be found in Scolaro et al. (2020) and Scolaro (2021).

As the main applications and validation efforts have focused mostly on base-irradiation conditions (Scolaro et al., 2022), the current version of OFFBEAT employs a small-strain mechanics solver. In this paper, the implementation of a finite strain mechanical framework in the code is described. In view of the participation of OFFBEAT to the EURATOM project OperaHPC (EURATOM, 2022), that aims to enhance the prediction capabilities of state-of-the-art fuel performance tools, such development represents a fundamental step to transition towards a mechanistic representation of multi-dimensional scenarios involving large deformations. In addition, the introduction of large strain capabilities in a finite volume code for nuclear application as OFFBEAT is of interest in the perspective of future high-fidelity multi-physics analysis

* Corresponding author.
E-mail address: edoardo.brunetto@epfl.ch (E.L. Brunetto).

https://doi.org/10.1016/j.nucengdes.2023.112232
Received 28 October 2022; Received in revised form 17 February 2023; Accepted 18 February 2023
Available online 4 March 2023

of accidental transients such as LOCAs, where the tight coupling with CFD or thermal hydraulic solvers (e.g. the GeN-Foam platform (Fiorina et al., 2015)), typically based on the same finite volume discretization method, becomes more relevant. This work reviews the main theoretical background behind the finite strain approach, detailing the implementation of the new mechanical solver and discussing the results of some analytical verification tests.

As one of the main applications of large-strain theory in fuel performance (Di Marcello et al., 2014; Pastore et al., 2021a; Pastore et al., 2021b), LOCA experiments are targeted for the validation of the newly developed OFFBEAT mechanical solver. The code is therefore provided with behavioral models and correlations tailored for the high-temperature accidental regimes typical of LOCA events. The introduced features comprehend correlations for high temperature creep, crystallographic Zirconium phase transition model and cladding burst criteria. The paper shows and discuss the validation results for the PUZRY separate-effect tests (Perez-Feró et al., 2010) as well as for the IFA-650.2 integral experiment (Ek, 2005). The data resulting from the two experiments are made available by the International Fuel Performance Experiments (IFPE) database ((NEA), 2022).

Other fuel performance codes have been previously extended to a finite strain formulation for analysis of accidental transients. The most notable examples include the introduction of a mono-dimensional logarithmic strain framework in ALCYONE (Helfer, 2015) and the extension to large-strain of the TRANSURANUS code (Di Marcello et al., 2014). In the case of the BISON fuel performance code, as it was provided with a finite strain mechanical framework since the beginning, the extension to LOCA analysis was focused mostly on the introduction and validation of high temperature models (Williamson et al., 2016).

The structure of this paper is described hereafter: the extension of the mechanical framework of OFFBEAT with the implementation of the large-strain solvers is shown in Section 2. The verification of the large-strain mechanical solver is detailed in Section 3, where the results of two verification test are shown. Section 4 provides an overview of the models for creep, cladding failure and Zircaloy phase transition implemented appositely for the LOCA regime. The Validation procedure against a separate-effect and an integral experiment is shown in Section 5, where OFFBEAT results are compared to experimental data and to BISON and TRANSURANUS calculations. Section 6 draws the conclusions and provides an overview of the work, outlining further code developments on the same research topic.

2. Extension of the OFFBEAT mechanical framework

The linear momentum conservation equation is the governing law of mechanics used to determine the stress and displacement distributions within a solid body. The law states that the sum of the forces acting on a solid body of volume Ω and surface Γ must be equal to its change of linear momentum (or inertia), and it is mathematically represented by Eq. (1):

$$\int_{\Omega} \rho \frac{\partial^2 \vec{D}}{\partial t^2} d\Omega = \oint_{\Gamma} (\boldsymbol{\sigma} \cdot \vec{n}) d\Gamma \tag{1}$$

where ρ is the body's density, $\vec{D}$ is the displacement vector field, σ is the Cauchy stress tensor and $\vec{n}$ is the unit vector normal to the body's surface. The presence of external body forces, such as those due to gravity, is disregarded in Eq. (1) for the sake of simplicity. The closure equation to relate the stress tensor σ with the displacement field $\vec{D}$ is provided by constitutive laws (e.g. Hooke's law of elasticity) in the form $\sigma = f(\boldsymbol{\varepsilon})$, where $\boldsymbol{\varepsilon}$ represents the strain tensor, typically calculated as $\boldsymbol{\varepsilon} = f(\nabla \vec{D})$. The integration domain in Eq. (1) corresponds to the body's current (or "deformed") geometrical configuration and in turn depends on the displacement fields itself.

2.1. The small-strain approximation

In many engineering applications of solid mechanics the deformations are significantly smaller than the characteristic dimensions of the examined body. In these circumstances one can neglect the geometric non-linearity and assume that the integration domain remains undeformed, simplifying the treatment of the governing equation by means of the small-strain approach. Under this approximation, the linear momentum equation (Eq. (1)) can be solved on the undeformed domain of volume Ω_0 and surface Γ_0 as shown by Eq. (2).

$$\int_{\Omega_0} \rho_0 \frac{\partial^2 \vec{D}}{\partial t^2} d\Omega_0 = \oint_{\Gamma_0} (\boldsymbol{\sigma} \cdot \vec{n_0}) d\Gamma_0 \tag{2}$$

In addition to the geometric linearity of the domain, the small-strain approach disregards higher order terms appearing in the definition of the strain tensor ε, which is expressed as a function of the deformation gradient $\boldsymbol{F} = \nabla \vec{D} + \boldsymbol{I}$ as shown in Eq. (3).

$$\boldsymbol{\varepsilon}_{small-strain} = \frac{1}{2}\left(\boldsymbol{F}^T + \boldsymbol{F}\right) - \boldsymbol{I} = \frac{1}{2}\left(\nabla \vec{D} + \left(\nabla \vec{D}\right)^T\right) \tag{3}$$

The resulting linear strain tensor represents only an approximate metric of strain, and gives inaccurate estimates when large body rotations are involved (i.e. it is not rotational-invariant). Despite there is no clear indication on the validity bounds of the small-strain approximation, a general rule-of-thumb in mechanics suggests considering it valid for engineering strains smaller than 1% (Van Uffelen et al., 2019).

2.2. The large-strain mechanical solver

Accidental transients of interest for fuel performance analysis are often characterized by the occurrence of large deformations. To extend the OFFBEAT application range to such scenarios, two different large-strain solvers are implemented in the code: a Total-Lagrangian and an Updated-Lagrangian solver. The two differ for the approach used to account for the domain geometric non-linearity (i.e. for the deformation of the computational domain). With the Total-Lagrangian method, the momentum conservation equation is still solved on the undeformed geometry with volume Ω_0 as shown in Eq. (4).

$$\int_{\Omega_0} \rho_0 \frac{\partial^2 \vec{D}}{\partial t^2} d\Omega_0 = \oint_{\Gamma_0} \left(J\boldsymbol{F}^{-T}\boldsymbol{v}\vec{n_0}\right) \cdot \boldsymbol{\sigma} d\Gamma_0 \tag{4}$$

In addition, Nanson's relation (i.e. $\vec{n} d\Gamma = J\boldsymbol{F}^{-T}\vec{n_0} d\Gamma_0$) are used to relate the initial area vector $\vec{n_0} d\Gamma_0$ with the deformed area vector $\vec{n} d\Gamma$, with J representing the Jacobian determinant of the deformation gradient (i.e. $J = \det(\boldsymbol{F})$).

With the Updated-Lagrangian method the computational domain is instead updated in time according to the deformation state of the body and the momentum balance equations are solved on the so-called "updated" configuration as shown in Eq. (5):

$$\int_{\Omega_u} \frac{\partial}{\partial t}\left(\rho_u \frac{\partial \vec{D}}{\partial t}\right) d\Omega_u = \oint_{\Gamma_u} \left(j\boldsymbol{f}^{-T} \cdot \vec{n_u}\right) \cdot \boldsymbol{\sigma} d\Gamma_u \tag{5}$$

where the Nanson's relationship ($\vec{n} d\Gamma = j\boldsymbol{f}^{-T} \cdot \vec{n_u} d\Gamma_u$) depends upon the relative deformation gradient $\boldsymbol{f}$ and its Jacobian determinant j. To be coherent with such approach, OFFBEAT updates the finite-volume mesh points at the end of each time-step. The displacement at the mesh points is obtained by linear interpolation of the cell-centered displacement field computed by solving the momentum balance equation. Further details on the dynamic mesh feature can be found in Brunetto et al. (2021).

Despite being equivalent from the mathematical point of view, the Total- and Updated- Lagrangian approaches can differ in terms of numerical performances. As documented in Cardiff et al. (2017), their

numerical implementation in a Finite Volume framework can produce some differences in robustness and convergence of a segregated solution algorithm. As a matter of fact, the use of a segregated algorithm requires the use of iterative traction boundary conditions, that are found to provide a more stable solution when the iterations runs over traction terms that depend of the relative deformation gradient (as in the case of the Updated-Lagrangian approach) rather than on the total deformation gradient (as in the Total-Lagrangian approach). In the cases examined for this paper, the updated Lagrangian solver has proven to be more stable and to provide better results for the mechanical analysis of bodies undergoing large deformations. For this reason, it is selected for the verification and validation procedures described in this work.

Besides addressing the geometric non-linearity, large-strain analysis requires a coherent formulation of the strain tensor. Hence, apposite large-strain tensor definitions are implemented in OFFBEAT. The main ones are the Green-Lagrange and the Euler-Almansi definitions of strain (see Eq. (6) and Eq. (7) respectively). The Green-Lagrange strain tensor $\boldsymbol{E}$:

$$\boldsymbol{E} = \frac{1}{2}\left(\boldsymbol{F}^T\boldsymbol{F} - \boldsymbol{I}\right) = \frac{1}{2}\left[\nabla\vec{\mathrm{D}} + \left(\nabla\vec{\mathrm{D}}\right)^T + \left(\nabla\vec{\mathrm{D}}\right)^T \cdot \nabla\vec{\mathrm{D}}\right] \tag{6}$$

is easily recognizable as the direct generalization of Eq. (3), the only difference being the presence of the non-linear term $\left(\nabla\vec{\mathrm{D}}\right)^T \cdot \nabla\vec{\mathrm{D}}$. Analogously to the small-strain tensor, $\boldsymbol{E}$ is a measure of the deformation of the body with respect to its initial configuration.

The Euler-Almansi strain tensor $\boldsymbol{e}$:

$$\boldsymbol{e} = \frac{1}{2}\left(\boldsymbol{I} - \boldsymbol{F}^{-T}\boldsymbol{F}^{-1}\right) = \frac{1}{2}\left[\nabla\vec{\mathrm{D}} + \left(\nabla\vec{\mathrm{D}}\right)^T - \left(\nabla\vec{\mathrm{D}}\right)^T \cdot \nabla\vec{\mathrm{D}}\right] \tag{7}$$

Is instead a metric for the deformation of the body with respect to its current configuration. The Green-Lagrangian and the Euler-Almansi formulations are therefore two different metrics for strain because of the different reference configuration considered (initial and deformed respectively), but they both reduce to the small-strain definition in case of infinitesimal deformations. Other options are also available in OFFBEAT (such as the Hencky strain) but will not be discussed in this scope.

2.3. Summary of the available mechanical solvers in OFFBEAT

OFFBEAT is currently equipped with four different mechanical solvers, listed in Table 1. They can be distinguished into "total" and "incremental" solvers depending on their main unknown being the total displacement field $\vec{D}$, or the incremental displacement $\overrightarrow{DD}_{\Delta t}$ occurring during the time step Δt. For updated solvers, the total displacement is computed as $\vec{D}_t = \vec{D}_{t-\Delta t} + \overrightarrow{DD}_{\Delta t}$, where $\vec{D}_{t-\Delta t}$ represents the displacement calculated at the end of the previous time step $t - \Delta t$. Despite being equivalent to total solvers from the mathematical viewpoint, incremental solvers are more practical for handling the mesh update. This is due to the mesh-motion algorithm implemented in OFFBEAT, which requires the incremental displacement field to update the location of the mesh points at the end of each time-step.

A "Small Strain Updated" solver has been implemented in OFFBEAT as an incremental variation of the traditional small-strain approach. This solver is provided with mesh-motion capabilities and solves the momentum continuity equation for the increment field $\overrightarrow{DD}_{\Delta t}$ while maintaining all the main assumptions of small-strain theory (i.e. absence of Nanson's formula and a linear strain tensor). The "Small Strain Updated" solver allows to account for geometric non-linearities in case of large deformation scenarios, but it is still limited in accuracy by a linear definition of the strain tensor and a simplified formulation of the momentum continuity equation. As summarized in Table 1, a wider selection of strain tensor definitions is instead available for the two large-strain solvers in OFFBEAT.

Table 1
Summary table of the mechanical solvers available in OFFBEAT.

Mechanical Solver	Solver Type	Mesh Update	Strain Tensor Definition
Small Strain	Total	×	Linear
Small Strain Updated	Incremental	✓	Linear
Large Strain Total-Lagrangian	Total	×	Euler-Almansi, Green-Lagrange, Hencky or Linear
Large Strain Updated-Lagrangian	Incremental	✓	Euler-Almansi, Green-Lagrange, Hencky or Linear

The mechanical solvers used by other fuel performance codes for large strain analysis are various. TRANSURANUS uses an hybrid approach similar to the one herein described as "Small Strain Updated", where the mechanical problem is solved through the small-strain approach with an updated geometry and Euler-Almansi strain tensor definition (Di Marcello et al., 2014). Instead, the mechanical solver used in BISON is based on a finite-strain Updated-Lagrangian approach (Williamson et al., 2012).

3. Verification of the large-strain solver

Two verification tests are run to evaluate the newly implemented finite-strain mechanics solver of OFFBEAT. The first verification case consists of an axisymmetric 1D thick-walled cylinder having an inner radius of 10 mm and an outer radius of 20 mm. A fixed displacement history is imposed at the inner radius, gradually increasing from 0 until a maximum displacement of 75 mm. The computational mesh used for the cylinder is a 1D wedge discretized with 80 cells along the radial direction and one-cell thick in the azimuthal direction (see the simplified scheme of Fig. 1b). The material properties are derived from a previous work where the same test-case was performed for similar verification purposes by Cardiff et al. (2017). The mechanical properties of the solid body given in the reference (i.e. Young's Modulus, Yield Stress and Shear Modulus) are appositely selected to cause a rigid plastic deformation, allowing the comparison of the calculated radial stresses with the exact analytical solution provided by Eq. (8).

$$\boldsymbol{\sigma_{rr}} = \left(\frac{\sigma_Y}{\sqrt{3}}\right)\ln\left(\frac{(r_0/a_0)^2 + (a/a_0)^2 - 1}{(b_0/a_0)^2 + (a/a_0)^2 - 1}\right) \tag{8}$$

In Eq. (8), σ_Y is the Yield Stress, a_0 and b_0 are the initial inner and outer radii, a and b are the current inner and outer radii and r_0 is the radial coordinate in the initial configuration at which the stresses are calculated.

For the analysis of this test-case a non-linear constitutive law is implemented and employed in OFFBEAT. The law, which consists of a Neo-Hookean plasticity model (see ref. Cardiff et al., 2018 for further details), provides a closure equation suitable to relate stress and strain in case of large deformations. Despite the use of such constitutive law is fundamental for this specific verification case where body deformations are brought to extreme, the experience matured in the framework of this work proves that the linear elasto-plastic constitutive law (i.e. Hooke's linear elasticity combined with Von Mises plasticity model (Cardiff et al., 2018)) represents a reasonable approximation for cases of interest in the nuclear fuel behavior field (see the validation cases of Section 5).

The results of the verification test are shown in Fig. 1a. The results of the Updated-Lagrangian large-strain solver show a good agreement with the analytical solution, proving the solver to be suitable for an accurate prediction of the radial stress all along the cylinder deformation history.

A second verification test is run in OFFBEAT to assess the conservation of the mesh volume when the large-strain solver is used. As demonstrated in Di Marcello et al. (2014), volume conservation can be violated by small-strain solvers when large-deformation cases are considered. The same computational setup of the first verification case is replicated for the second test, but this time the maximum displacement

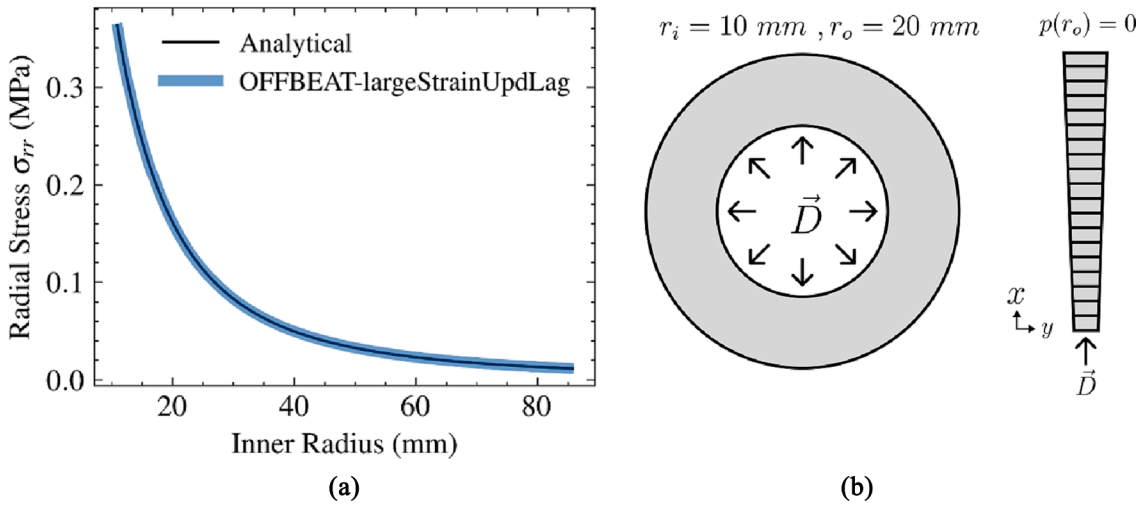

Fig. 1. Comparison of the OFFBEAT Updated-Lagrangian Large-Strain Solver against analytical solution for the radial stress at the inner radius (a) together with a simplified scheme of the geometry and the computational mesh used for the calculation (b).

of the cylinder inner radius is limited to a value of 30 mm. The simulation is repeated with three different mechanical solvers: the traditional "Small Strain" solver, the "Small Strain Updated" solver and the "Updated-Lagrangian Large Strain" solver. The comparison between the solvers is provided in Fig. 2, where the evolution of the total mesh volume (normalized to its initial value) is plotted against the updated internal radius r_i normalized with respect to the initial radius R_i. The calculation results show how the traditional small-strain solver violates the volume conservation as soon as the deformations grow larger than a few percent, and eventually leads to a failure of the simulation before the end of the deformation history. On the other hand, the incremental-updated version of the small-strain solver shows significantly smaller deviations, that reach a maximum value of ~4% at the end of the deformation history. The (small) discrepancies are imputable to the remaining approximation of the solver i.e. the lack of Nanson's formulae and the linear formulation of the strain tensor. Indeed, the use of the updated large-strain solver shows consistent volume predictions even at larger deformations.

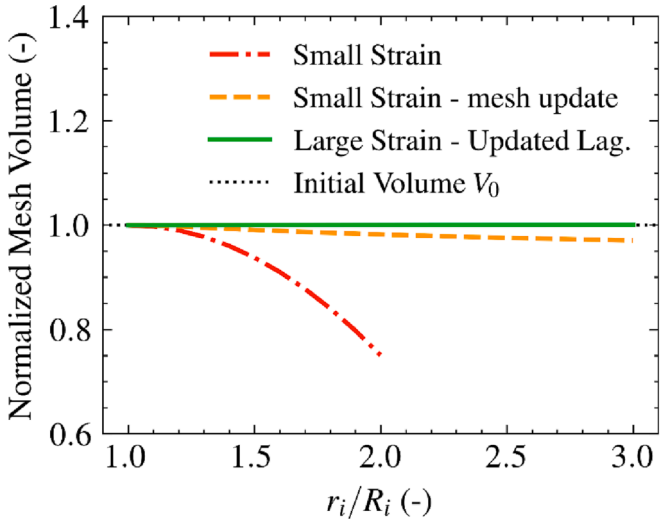

Fig. 2. Volume conservation check at large deformations with different OFFBEAT mechanical solvers.

4. Cladding models for LOCA analysis

During a LOCA the postulated loss of cooling causes the cladding temperature to rise well beyond the normal operational range. This leads to an increase in rod internal pressure, which in turn contributes to a sudden outward deformation of the cladding known as ballooning. As soon as the ballooning deformations overcome the material resistance capabilities, cladding fracture (i.e. burst) can occur. Accidental transients are characterized by Peak Cladding Temperatures (PCT) that can increase from an average operational value of ~600 K to a maximum of about 1300–1400 K. The high temperature regime causes the onset of specific phenomena which are normally negligible (or non-existent) in a nominal operation regime. To account for these phenomena, fuel performance codes like BISON (see Williamson et al., 2016) have identified specific models to be implemented for the analysis of high-temperature cladding behavior. Among these, a high-temperature thermal creep correlation, a Zirconium β-phase transition model and a burst failure model are implemented in OFFBEAT and described in the current section.

4.1. High temperature thermal creep

For standard operating conditions, OFFBEAT applies the creep model developed by Limbäck and Andersson (1996) for Zircaloy cladding. This model provides the creep rate as a combination of primary and secondary creep rate, where the secondary creep rate is in turn obtained by summing a thermal-induced and an irradiation-induced component. The validity of this model is limited to temperatures below 700 K.

The OFFBEAT Zircaloy creep model is extended to high temperature conditions by following the work of Pastore et al. (2021b). The model defines three different temperature regimes:

- A normal operation regime for temperatures below 700 K;
- A high temperature regime for temperatures above 900 K;
- A transitional regime for temperature between 700 and 900 K.

Different creep rate correlations are used for the low- and high-temperature regimes, while a linear interpolation is used to evaluate the creep rate in the transitional regime. Below 700 K, the standard Limbäck model is used, while the high temperature creep strain rate correlation has the form of a Norton power equation, as shown in Eq. (9):

$$\dot{\varepsilon}_{creep} = A\exp\left(-\frac{Q}{RT}\right)\sigma_{eff}^{n} \tag{9}$$

where $\dot{\varepsilon}_{creep}$ is the effective creep strain rate, A is a strength coefficient expressed in $MPa^{-n}s^{-1}$, Q is the activation energy expressed in $\frac{J}{mol}$, T is the temperature, σ_{eff} is the effective Von Mises stress in MPa, and n is a dimensionless correlation parameter. The value of A, Q and n depend upon the volumetric fraction of β-phase present in Zircaloy, for which a specific model is introduced (see following subsection).

The simulation of a LOCA requires some caution in the choice of time-step size. In the case of a ballooning event the creep rates are particularly high and small time steps are necessary for an accurate description of the cladding deformation dynamics and for stabilizing the highly non-linear stress–strain relation. Adaptive time-stepping scheme based on a user-defined maximum creep strain increment can be used in OFFBEAT simulations. For the cases analyzed in this text, time-steps in the order of magnitude of 10^{-3} seconds have been deemed adequate to the study of cladding ballooning.

4.2. Beta phase transition model

Beyond an onset temperature of around 1080 K, the hexagonal crystal structure (i.e. α-phase) of Zircaloy progressively transitions towards a more stable cubic crystal structure (i.e. β-phase). The dynamics of this transition depends mainly on the heating or cooling rate of the cladding. One of the main effects of the crystallographic transition from α- to β-phase is the enhancement of the thermal creep rate.

OFFBEAT has been provided both with a static and a dynamic model for the β-phase transition of Zircaloy. The static model, derived from Forgeron et al. (2000), is valid when the kinetics of the transition can be neglected (i.e. during slow temperature transients) and consists of a simple correlation that relates the local cladding temperature T to a specific β-phase volumetric fraction y_{eq}. The Forgeron's equation is expressed by means of Eq. (10):

$$y_{eq} = 1 - e^{-[C\cdot(T-T_0)]^n} \tag{10}$$

where C, T_0 and n are correlations parameters that are material dependent.

For the study of LOCA transients, where temperature ramps in the cladding are generally fast, a better estimation of the volumetric fraction of β-phase is typically obtained through a dynamic phase transition model. According to the model by Massih (2009) implemented in BISON (Pastore et al., 2021b), the evolution of the volumetric fraction of β-phase in Zircaloy is governed by the differential equation shown in Eq. (11):

$$\frac{dy}{dt} = k(T)\left[y_{eq}(T) - y\right] \tag{11}$$

where y is the volumetric fraction of β-phase, k is a rate parameter expressed in s^{-1} and y_{eq} is the equilibrium value of y. Both k and y_{eq} depend on the temperature rate of change, thus allowing the dynamic model to more accurately reproduce the kinetics of the production of β-phase. The difference between the static and dynamic approaches can be visualized in Fig. 3, that shows the verification of the model implemented in OFFBEAT against the reference model by Massih (2009).

4.3. Burst models

The accurate prediction of the moment of cladding failure during a LOCA transient is of primary importance for fuel performance analysis. The assessment of cladding burst occurrence is performed by means of simplified burst criteria rather than with fracture dynamics, which would require an accurate modeling of fractures propagation and therefore a significant computational overhead to fuel performance computations. In the framework of this work, OFFBEAT is provided with two different failure criteria derived from BISON (Idaho National Laboratory, n.d.) for the Zircaloy material: an overstrain criterion and a plastic instability criterion. According to the first criterion, the cladding is considered to fail as soon as the radially-averaged creep hoop strain (expressed as engineering strain) overcomes the limit of 40%. Analogously, the plastic instability criterion the material considers the material to fail when the radially-averaged effective plastic strain rate reaches a limiting value of $2.78{\cdot}10^{-2}s^{-1}$. The introduction of additional failure criteria, such as the overstress criterion or the strain energy density model, is planned as a part of the future code development activities.

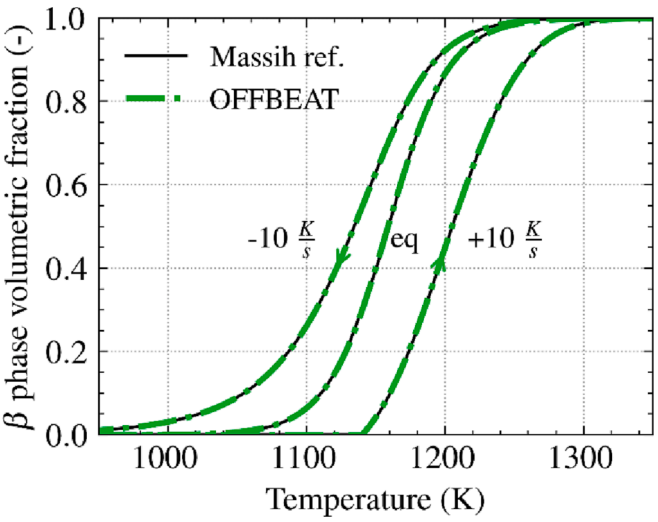

Fig. 3. Verification of the OFFBEAT model for β-phase transition of Zirconium compared to the model from Massih. The curve shown in the plot are obtained for a hydrogen concentration of 0 ppm.

5. Code validation: Application to ballooning experiments

The newly developed OFFBEAT finite strain solver is validated against two experiments made available by the IFPE database ((NEA), 2022), namely the PUZRY experimental series (Perez-Feró et al., 2010) and the IFA-650.2 in-pile test (Ek, 2005). The experiments consist respectively of a separate-effect and an integral test under simulated LOCA conditions. The occurrence of ballooning deformations and eventually rod burst is observed in the experimental specimens for both cases. Quantities of interest such as the burst time, the inner rod pressure and the cladding profilometry are monitored during the course of the experiments. The two cases differ for their experimental setup and methodology: in the PUZRY case, Zircaloy tubes samples were subjected to different pressure ramps while kept in isothermal conditions until ballooning and burst eventually occurred. The IFA-650.2 experiments consisted instead of a more complicated experimental setup, where a fresh pressurized PWR rod was used in an experimental rig appositely designed to simulate LOCA conditions. Such experiments, which details are given in the respective dedicated subsections, are deemed of peculiar interest to evaluate the OFFBEAT prediction capabilities in the framework of postulated accident analysis. Moreover, the literature availability about fuel performance analyses on the same experiments (see Di Marcello et al., 2014; Pastore et al., 2021b and Pastore et al., 2021a) allows to compare the predictions of OFFBEAT with those of other fuel performance codes.

5.1. The PUZRY experimental series

PUZRY experiments (Perez-Feró et al., 2010) are part of the separate-effect tests on cladding ballooning performed at the Atomic Energy Research Institute of the Hungarian Academy of Sciences. With the objective of testing the mechanical response of cladding material in

LOCA scenarios, the experiments were carried over in a non-corrosive environment on 31 identical Zircaloy-4 samples subjected to inner pressure ramps of different worth until occurrence of ballooning and burst. The specimens consisted of 50-mm high cladding tubes closed at both ends with end plugs. Inner and outer diameter of the samples were respectively 9.3 mm and 10.75 mm. The specimens, initially kept at a constant pressure of 0.1 MPa in a quartz tube filled with Argon, were then subjected to internal pressure ramps by means of a pipe passing through one of their ends. The experiment was continued until burst while monitoring the temperature and pressure histories. The tests covered a range of temperatures from 970 K to 1475 K and a range of pressurization rates from $4.8{\cdot}10^{-4}$ MPa/s to $2.6{\cdot}10^{-2}$ MPa/s. Further details on the experimental setup are given in Perez-Feró et al. (2010).

5.1.1. Simulation setup

Thirty-one OFFBEAT simulations are run to replicate all the experiments of the PUZRY series. The way the simulations are built is analogous to what was done in the scope of a previous work performed with the BISON code (Pastore et al., 2021b). The OFFBEAT simulations are run using 2D axisymmetric r-zeta models of the samples. Because of the axial symmetry of the problem, only the lower half of the sample length is modeled, and symmetry boundary conditions for the thermal and the mechanics solver are used on the surface corresponding to the half-length plane. The bottom end plug is not explicitly modeled and it is accounted for by means of a zero-displacement mechanical boundary condition. The inner pressurization of the sample is modeled through a mechanic boundary condition imposing a time-dependent pressure history. The outer surface of the sample is instead kept at the constant initial pressure of 0.1 MPa. The thermal boundary conditions consist of a time-dependent imposed temperature profile on the outer surface of the specimen and a zero-gradient boundary conditions for all the other surfaces. Accordingly to what was done in a previous work of Pastore et al. (2021b), all the simulations were performed starting from a constant temperature of 300 K and a constant internal pressure of 0.1 MPa. Then, by keeping a constant pressure, the temperature is raised over a period of 1000 s up to the specific value for the experiment. After the temperature is stabilized, the pressurization is applied at constant temperature until the rupture of the cladding is predicted by the code. The OFFBEAT simulations are run with the large-strain updated-Lagrangian mechanical solver, enabling the high-temperature creep model and Zircaloy phase-transition model described above. The over-strain burst criterion with a threshold of 40% (engineering strain) on creep hoop strain is used to evaluate the cladding failure.

5.1.2. Validation results

The OFFBEAT results relative to the time of burst of the PUZRY experiments are depicted in Fig. 4 and Fig. 5, and show a general good agreement with experimental data and with the results obtained with the BISON fuel performance code in Pastore et al. (2021b). From Fig. 4 it is noticeable that the larger discrepancies are represented by points lying below the C = E line, and therefore represent an under-estimation of the time of burst (i.e. a conservative estimation). From Fig. 5 the higher discrepancies are observed for temperatures lower than 1250 K, and are particularly large for the points below 1050 K.

As explained by the authors of Pastore et al. (2021b), the motivations for these deviations can be partly found in the uncertainty of the high-temperature creep correlation and partly in the anisotropic behavior of the α-phase of Zircaloy. The temperatures in the range 1050 K-1250 K correspond indeed to the coexistence of α and β phase of Zircaloy at equilibrium, which is the region interested by largest uncertainties of the high temperature creep model. On the other hand, the temperatures below 1050 K correspond to pure α-phase of Zircaloy, which is notably characterized by a strong anisotropic behavior (see Pastore et al., 2021b and the references herein cited) which is not contemplated in the current OFFBEAT implementation.

Another quantity of interest considered for the validation of the

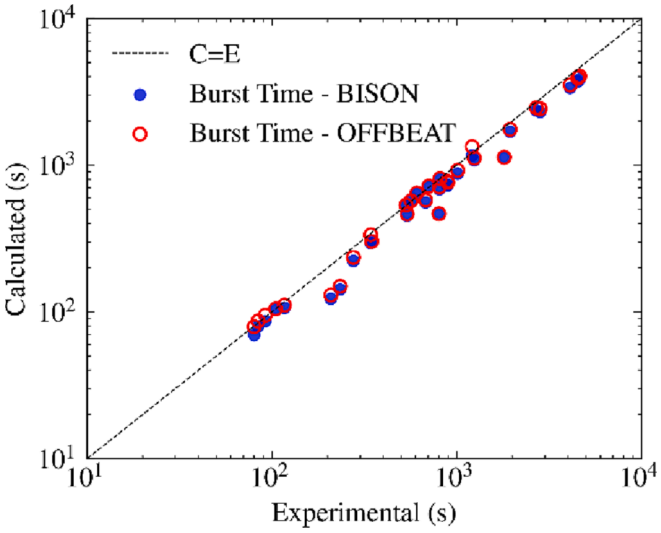

Fig. 4. Comparison between experimental and measured time of burst for the PUZRY samples.

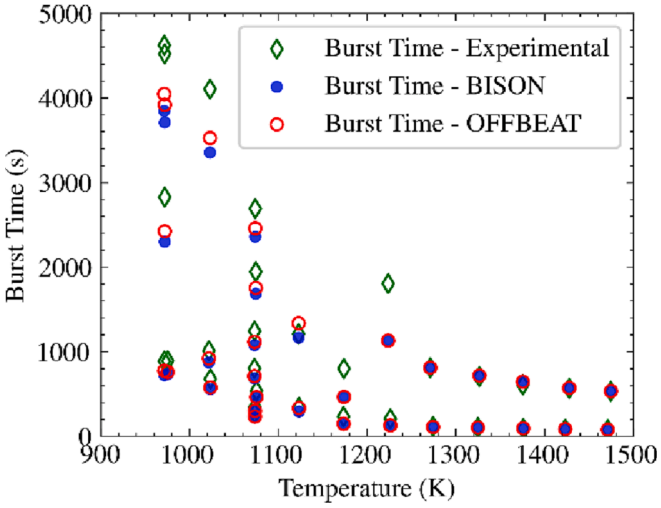

Fig. 5. Experimental and computed burst time as a function of temperature for the PUZRY samples.

PUZRY experiments is the maximum hoop strain at burst. As done in the framework of the FUMAC modeling benchmark (Pastore and Kulacsy, 2018), only six of the PUZRY specimens are selected for this comparison, namely the ones more representative of a large-break LOCA scenario. The OFFBEAT simulations for this comparison are run using both the overstrain and the plastic instability model as failure criteria to evaluate the occurrence of the cladding burst. The results of the simulations are collected in Fig. 6, where a relevant discrepancy is found between experimental and computational results. Both the overstrain and the plastic instability results are found to underestimate the maximum hoop deformation at burst. Similar discrepancies have been noticed in the framework of the FUMAC benchmark, where large differences were found across different codes' results. The benchmark results showed that the burst failure criteria are affected by large uncertainties, making the prediction of cladding strain at burst difficult for fuel performance codes. This difficulty is dictated by the high strain rates that characterize the ballooning dynamics, where a small underprediction of the burst time can cause a relevant underprediction of the cladding strain. In addition, when comparing calculated and experimental burst strains one should always consider the additional deformation happening in the

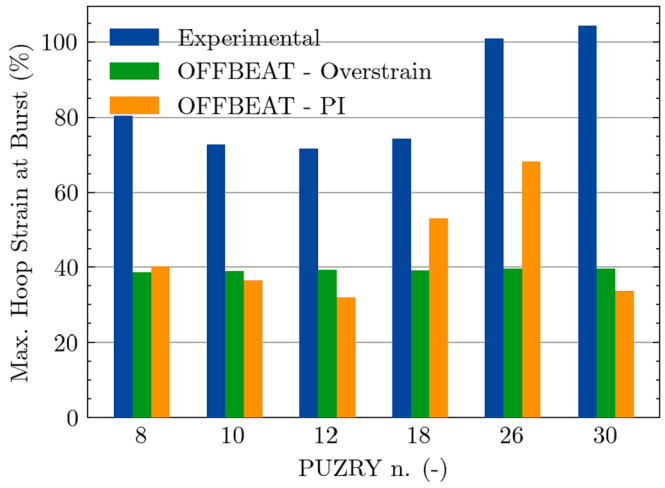

Fig. 6. Comparison of maximum hoop strain at burst instant as evaluated by the different criteria available in OFFBEAT against experimental measurements.

instants that follow the onset of the cladding rupture, that is not explicitly simulated in state-of-the-art fuel performance code. However, better estimations of the time-of-burst strains could be obtained by taking into account the anisotropic behavior of the α-phase of Zircaloy or by using more mechanistic failure criteria.

5.2. The IFA-650.2 experiment

The IFA-650.2 integral experiment has been carried out with the specific purpose of maximizing the cladding ballooning deformation of a fresh UO_2 fuel rod, eventually provoking its burst. The 50 cm long fuel rod, whose specifics are given in Table 2, was located in a high-pressure flask connected to a 70 bar heavy water loop and a blowdown system. During the normal operation of the rod, the rig was connected to the high-pressure loop, while the loss of coolant event was simulated bypassing the rig and letting the coolant flow through the blowdown system to a shielded tank, with a pressure of about 2 bar. To simulate the heat from neighboring fuel rods, the experimental assembly was provided with an electrical heater of the same height of the fuel stack. The heater was placed inside the high-pressure flask and surrounded the rod as a part of a flow separator. The heater and reactor power influenced the cladding temperatures. The experiment was started with a preparatory phase, where the fresh UO2 was irradiated at a Linear Heat Rate (LHR) of 10 kW/m for 1.5 days to crack the fuel pellets and a forced circulation regime was maintained in the high-pressure loop. This high-power irradiation phase was then followed by a linear power decrease which brought the LHR to a value of 2.3 kW/m at around 21 min prior to the blowdown. Once the low-power level was reached, the heater was turned on at a power of about 1.8 kW/m, i.e. the value previously determined during test calculations to reach a target Peak Cladding Temperature (PCT) of 1050 °C. About 2 min before the blowdown the outer loop was disconnected from the experimental rig of which the pressure flask is part, and the flow separator enabled the onset of a natural convection flow. The blowdown was subsequently provoked by the opening of dump valves, and the rig was emptied within 30 – 40 s.

Table 2
Geometrical details of the IFA-650.2 experimental rod.

Active fuel length	500 mm
Pellet outer diameter	8.29 mm
Pellet height	8.00 mm
Cladding outer diameter	9.50 mm
Cladding thickness	0.57 mm
Diametral gap clearance	0.07 mm
Total free gas volume	17.40 cm^3

The lack of coolant in the rig caused a sudden temperature increase in the cladding, leading eventually to the target PCT of 1050 °C. During the cladding heat up phase ballooning and burst occurred. The reactor scram and the shutdown of the electrical heater occurred around 6 min after the estimated time of burst. Further details on the experimental setup can be found in the technical report of the experiment (Ek, 2005).

5.2.1. Simulation setup

A 2D radial-axial (r-z) computational model of the IFA-650.2 experimental rod is used in OFFBEAT, taking advantage of the azimuthal symmetry of the problem. An additional modeling assumption is introduced by considering the whole fuel stack as a smeared column of fuel material. This choice is motivated by the focus of the current analysis, oriented toward the prediction of integral quantities rather than local phenomena involving the pellet geometry (e.g. ridging). To further reduce the computational domain, the upper plenum of the rod is only partially modeled. Only 40 mm in height above the quote of the fuel top surface are modeled in the rod geometry while the remaining portion is accounted for by OFFBEAT as part of a virtual gas reservoir with prescribed time-dependent temperature and pressure histories. The computational mesh used for the calculations in OFFBEAT is shown in Fig. 7, where the reference (i.e. initial) configuration is shown together with the deformed configuration at the moment of burst.

The thermo-mechanical boundary conditions set in OFFBEAT to simulate the IFA-650.2 rod are mainly derived from the experimental measurements made available in the IFPE database. From the mechanical point of view, the following boundary conditions are imposed:

- A time dependent uniform pressure on the outer side of the cladding, deriving from the coolant pressure measurements of the IFA.650.2 experiment;
- A fixed zero-displacement is imposed at the bottom surfaces of fuel and cladding, assuming that realistically zero or little displacement will affect these parts of the rod;
- At the top fuel surface an apposite boundary condition is imposed to account for the balance of all the forces acting on it (i.e. plenum

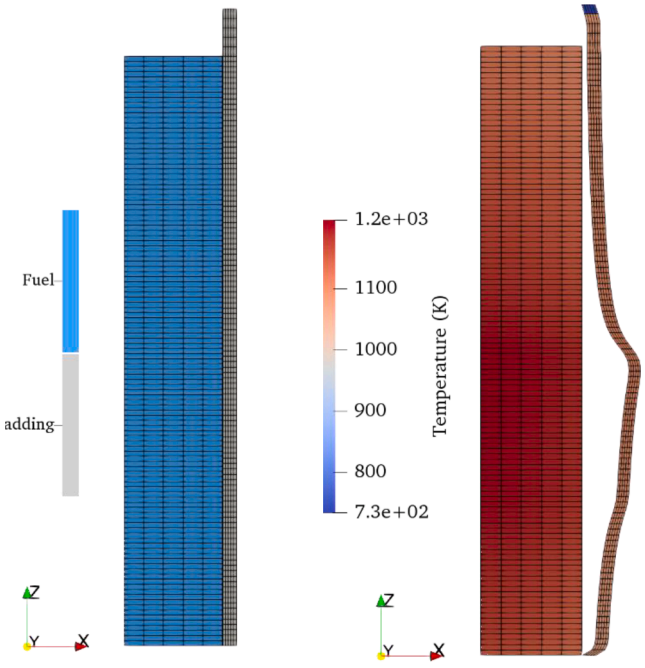

Fig. 7. Computational mesh of the IFA-650.2 rod in its initial (left) and deformed (right) configuration. The deformed state shown in the figure is correspondent to the estimated moment of burst. For visualization purposes, the meshes are warped 20x in the x-direction.

spring, inner rod gas etc.). The same goes for the top cladding surface, where also the pressure imposed by the coolant is accounted in the force balance;
- The mechanical interaction of fuel and cladding within the gap is managed by a boundary condition that allows mechanical contact between the two. The initial pressure of the inner rod gas is also part of the data provided by IFPE.

For what concerns thermal boundary conditions instead:

- A time-dependent temperature axial profile, derived from the data available in the IFPE database, is imposed to the outer cladding surface;
- For the fuel-cladding gap, an OFFBEAT specific boundary condition to account for the heat exchange contributions coming from gas conduction, irradiation and solid conduction (only in case of contact) is set;
- The boundary conditions for top and bottom surfaces of the rod are set to zero-gradient.

While the implementation of boundary conditions has been effortless in most cases (e.g. time-dependent coolant pressure on the cladding outer surface), other cases where the measured data were lacking or not satisfactory required some pre-processing. The temperature profile imposed at the outer surface of the cladding is an example of the latter because of the lack of experimental thermocouples measurements, which were available at two axial locations only (i.e. 100 and 400 mm of elevation with respect to the bottom fuel surface). To obtain an axial profile with a better spatial discretization in correspondence of the cladding portion facing the fuel stack, the procedure detailed in Pastore et al. (2021a) is followed, with the only difference being the linear interpolation scheme used in the work at hand instead of a quadratic spline. The temperature profile is then extended up to the top of the modeled portion of the cladding, assigning a constant temperature up to 10 mm above the top fuel surface and then a linear variation of temperature that reaches the value of the outlet coolant temperature in correspondence of the top surface of the cladding. The temperature history assigned to the plenum reservoir coincides as well with the one registered by the thermocouple at the coolant outlet. The time progression of the simulation has been controlled with an automatic time-stepping algorithm based on the maximum allowed increment of creep strain between two subsequent steps. Such a criterion is fundamental to obtain a reliable solution for ballooning transients that are characterized by strong deformation rates. For the case at hand, a maximum allowed increase of 1e-4 has been selected, resulting in a minimum time step size in the order of magnitude of 1e-3 s. Other tests with a more restraining time step criterion on creep of 1e-5 have shown similar results and much longer computational times, therefore the value of 1e-4 has been deemed appropriate for the simulations. The OFFBEAT simulation is run from the beginning of the irradiation until the cladding rupture, which is predicted by the overstrain burst criterion model.

5.2.2. Validation results

The rod internal pressure and the cladding profilometry at time-of-burst are the two OFFBEAT outputs selected as quantities of interest for the code validation against the IFA-650.2 test. The results, summarized hereafter, are compared with the results obtained by TRANSURANUS and BISON in previous works (Di Marcello et al., 2014; Pastore et al., 2021a). Fig. 8 compares the online measurements of inner rod pressure in the seconds following the rig blowdown with the different codes predictions. The experimental data are plotted in the figure just until the moment of burst, i.e. until the instant preceding the drastic pressure drop caused by the cladding burst. During the first ~ 40 s after blowdown a decrease in the rod internal pressure is recorded by the pressure transducer. This is caused by the increased velocity of the water flowing outside the rig, that enhances the heat transfer with the fuel rod and therefore results in a decreasing temperature (and pressure). Consequently, the cladding heat up phase starts. This phase is characterized by a rapid rise of cladding temperature caused by the lack of cooling, which therefore results in a pressure increase. While the temperature continues to increase, about 80 s after blowdown the pressure ceases to increase due to the beginning of the ballooning phase. Due to the extreme temperatures reached by the cladding (over 1000 K), the last phase is characterized by large outward creep deformations (i.e. ballooning) that cause a dramatic pressure drop followed by the cladding rupture around 99 s after blowdown.

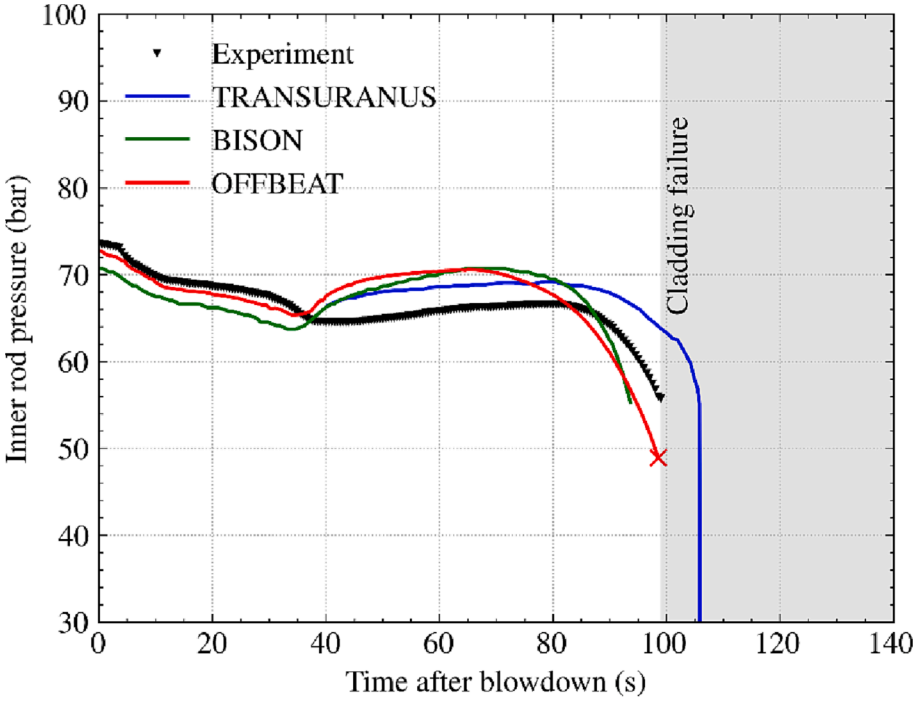

Fig. 8. Inner rod pressure behavior in the seconds after the rig blowdown up to the burst moment.

The rod inner pressure behavior predicted by OFFBEAT shows an overall qualitative agreement with the experimental data. Discrepancies with the experimental measurements and with the BISON calculation are minimal until ~ 40 s after blowdown, while TRANSURANUS data from Di Marcello et al. (2014) are not available for this phase. Discrepancies grow larger starting from the beginning of the pressure rise. In this phase, all the fuel performance codes overestimate the rod pressure. As suggested in Pastore et al. (2021a), this inaccuracy can be motivated by the multiple assumptions made to simplify the case, such as modelling the whole inner rod free volume as a single upper plenum or imposing to the upper plenum temperature the value recorded by the outlet coolant thermocouple. The mentioned assumptions are coherent to the ones made for the BISON simulation, and therefore explain the similar behavior of the two codes during the blowdown transient.

The time-of-burst prediction of OFFBEAT is in excellent agreement with the experimental observations, and it is estimated to happen after 99 s from the rig blowdown. The discrepancy with the BISON prediction, that estimates the burst to happen ~ 5 s before the experimental one, is probably to be imputed to the small variations in the outer cladding temperature profiles. The time-of-burst prediction, which is estimated by the two codes with an over-strain criterion, depends upon the maximum cladding deformation occurring during the ballooning transient. In this case, as the cladding deformation is essentially driven by the thermal creep strains, the deformation dynamics is extremely sensitive on the time-evolution of the temperature profile imposed on the cladding outer surface. For this reason, larger discrepancies are observed with respect to the pressure prediction of TRANSURANUS, which uses a temperature axial profile obtained by means of thermo-hydraulic calculations (Di Marcello et al., 2014) which is substantially different from the one used in OFFBEAT and BISON calculations.

Fig. 9 shows the outer profile of cladding at the time-of-burst as computed by fuel performance codes and compared to the Post Irradiation Examination (PIE) measurements.

All the codes predictions show a good quantitative estimation of the maximum cladding deformation at the burst moment, with a maximum diameter of ~ 13 mm reached right before rupture. The burst location, which correspond to the point of maximum strain in the codes results, is well predicted by the three codes with a slightly better performances shown by the OFFBEAT and BISON calculations. Once again, this is probably caused by the thermal boundary condition imposed on the outer cladding, which in the case of BISON and OFFBEAT causes the deformation to be larger in the lower half-plane of the rod. In said region, although slightly over-estimating the cladding deformation, the OFFBEAT results show a good qualitative description of the cladding profile.

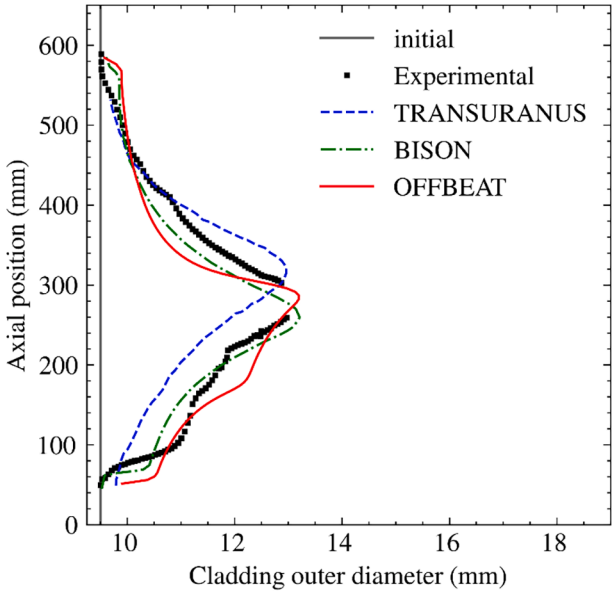

Fig. 9. Cladding profilometry at the burst moment.

Although mainly due to the practical impossibility to know the exact temperature profile evolution on the outer surface of the cladding, the discrepancies with the experimental profile can be imputable to several reasons. First of all, as the PIE measurements are carried over in cold conditions, minor differences on the rod thermal deformation are expected to exist with respect to the moment of burst (where temperature higher than 1000 K are reached by the cladding). In addition, because of the negligible amount of β-phase Zirconium estimated at the end of the simulation, the cladding is mainly composed by α-phase Zircaloy. Because of its hexagonal-close packed structure, the highly anisotropic mechanical properties of α-phase Zircaloy (not accounted for in the current OFFBEAT implementation) can be identified as source of discrepancy with respect to the experimental data.

6. Conclusions

The implementation in the OFFBEAT fuel performance code of a new mechanical framework suitable for finite deformations has been presented. The main motivation for this work was to enable OFFBEAT for the analysis of accidental scenarios, which are often characterized by the occurrence of large deformations in the fuel rod. Such extension has been performed through the implementation of new mechanical solvers in the code, provided with finite-strain formulations of the solid mechanics governing equation. In addition, apposite large strain definitions for the strain tensor have been implemented in OFFBEAT. This development is relevant for the code, as it allows to step beyond the classical small strain formulation commonly applied when dealing with base irradiation analyses.

Verification tests were performed to assess and demonstrate the correctness of the newly implemented mechanical solvers, showing good agreement with analytical results and improved accuracy with respect to the pre-existing small-strain solver in case of large deformations.

First validation efforts were carried out by analyzing two experiments performed in the past to simulate Loss of Coolant Accident conditions: the PUZRY separate-effect experiments and the IFA-650.2 integral test. For the sake of this validation, apposite models and correlations tailored for LOCA temperatures regime were introduced in the code. For both cases, the validation has demonstrated good prediction capabilities of the OFFBEAT fuel performance code, showing good agreement with experimental data and a response consistent with the predictions of other fuel performance codes where similar models and capabilities have been already implemented.

The discrepancies observed with respect to the experimental measurements are mainly imputable to the unavailability of key parameters for the simulated rods, such as an accurate temperature profile on the outer surface of the cladding. Other possible reasons have been identified, such as the absence of models accounting for the mechanical anisotropy of α-phase Zircaloy, or the uncertainties of the high-temperature creep model in the temperature range characterized by the coexistence of α and β Zirconium phases.

Future development activities for OFFBEAT will be oriented to further extend the code capabilities and applicability to off-normal conditions. For instance, models for high-temperature cladding oxidation and hydrogen pick-up in Zircaloy might be implemented in the future for a more accurate representation of the cladding behavior in the post-LOCA phase. Other developments to improve the predictions for the mechanical response of Zircaloy might include the previously mentioned models for the anisotropy of the α-phase, together with more mechanistic burst models.

CRediT authorship contribution statement

Edoardo Luciano Brunetto: Conceptualization, Methodology, Software, Visualization, Writing – original draft. **Alessandro Scolaro:** Supervision, Software, Writing – review & editing. **Carlo Fiorina:** Supervision, Writing – review & editing. **Andreas Pautz:** Project administration, Funding acquisition.

Declaration of Competing Interest

The authors declare that they have no known competing financial interests or personal relationships that could have appeared to influence the work reported in this paper.

Data availability

The verification cases illustrated in this paper are available in the public GitLab repository of OFFBEAT (https://gitlab.com/foam-for-nuclear/offbeat). The experimental data used for the validation procedure are instead accessible upon request through the International Fuel Performance Experiments (IFPE) database of the Nuclear Energy Agency (NEA).

References

(NEA), N.E.A., 2022. International Fuel Performance Experiments (IFPE) database [WWW Document]. URL https://www.oecd-nea.org/jcms/pl_36358/international-fuel-performance-experiments-ifpe-database (accessed 3.22.22).

Brunetto, E.L., Scolaro, A., Fiorina, C., Pautz, A., 2021. First Steps towards Large Strain Analysis in OFFBEAT. In: ANS Winter Meeting 2021. https://doi.org/doi.org/10.13182/T125-36858.

Cardiff, P., Karač, A., de Jaeger, P., Jasak, H., Nagy, J., Ivanković, A., Tuković, Ž., 2018. An open-source finite volume toolbox for solid mechanics and fluid-solid interaction simulations 1–45.

Cardiff, P., Tuković, Ž., Jaeger, P.D., Clancy, M., Ivanković, A., 2017. A Lagrangian cell-centred finite volume method for metal forming simulation. Int. J. Numer. Methods Eng. 109 (13), 1777–1803.

Di Marcello, V., Schubert, A., van de Laar, J., van Uffelen, P., 2014. The TRANSURANUS mechanical model for large strain analysis. Nucl. Eng. Des. 276, 19–29. https://doi.org/10.1016/J.NUCENGDES.2014.04.041.

Ek, M., 2005. LOCA Testing at Halden; The second experiment IFA-650.2 - OECD Halden Reactor Project. Norway.

EURATOM, 2022. OperaHPC - OPEN HPC THERMOMECHANICAL TOOLS FOR THE DEVELOPMENT OF EATF FUELS [WWW Document]. accessed 1.16.23. https://www.operahpc.eu/.

Fiorina, C., Clifford, I., Aufiero, M., Mikityuk, K., 2015. GeN-Foam: A novel OpenFOAM® based multi-physics solver for 2D/3D transient analysis of nuclear reactors. Nucl. Eng. Des. 294, 24–37. https://doi.org/10.1016/J.NUCENGDES.2015.05.035.

Forgeron, T., Brachet, J.C., Barcelo, F., Castaing, A., Hivroz, J., Mardon, J.P., Bernaudat, C., 2000. Experiment and modeling of advanced fuel rod cladding behavior under LOCA conditions: Alpha-beta phase transformation kinetics and EDGAR methodology, in: ASTM Special Technical Publication. https://doi.org/10.1520/stp14303s.

Geelhood, K., Luscher, W., Raynaud, P., Porter, I., 2015. FRAPCON-4.0: A Computer Code for the Calculation of Steady-State, Thermal-Mechanical Behavior of Oxide Fuel Rods for High Burnup. Richland, Washington 99352.

Helfer, T., 2015. Extension of monodimensional fuel performance codes to finite strain analysis using a Lagrangian logarithmic strain framework. Nucl. Eng. Des. 288, 75–81. https://doi.org/10.1016/J.NUCENGDES.2015.02.010.

Idaho National Engineering Laboratory, 1979. MATPRO - Version 11. A Handbook of Materials Properties For Use In The Analysis of Light Water Reactor Fuel Rod Behavior.

Idaho National Laboratory, n.d. Source Documentation | BISON [WWW Document]. URL https://mooseframework.inl.gov/bison/source/ (accessed 7.27.22).

Jiang, W., Singh, G., Hales, J.D., Toptan, A., Spencer, B.W., Novascone, S.R., Dhulipala, S.L.N., Prince, Z.M., 2022. Efficient high-fidelity TRISO statistical failure analysis using Bison: Applications to AGR-2 irradiation testing. J. Nucl. Mater. 562, 153585. https://doi.org/10.1016/J.JNUCMAT.2022.153585.

Limbäck, M., Andersson, T., 1996. A model for analysis of the effect of final annealing on the in- and out-of-reactor creep behavior of zircaloy cladding. ASTM Spec. Tech. Publ. 1295, 448–468. https://doi.org/10.1520/stp16185s.

Massih, A.R., 2009. Transformation kinetics of zirconium alloys under non-isothermal conditions. J. Nucl. Mater. 384, 330–335. https://doi.org/10.1016/J.JNUCMAT.2008.11.033.

Pastore, G., Gamble, K.A., Williamson, R.L., Novascone, S.R., Gardner, R.J., Hales, J.D., 2021a. Analysis of fuel rod behavior during loss-of-coolant accidents using the BISON code: Fuel modeling developments and simulation of integral experiments. J. Nucl. Mater. 545, 152645 https://doi.org/10.1016/j.jnucmat.2020.152645. ISSN 0022-3115.

Pastore, G., Kulacsy, K., 2018. IAEA FUMAC Benchmark of Fuel Performance Codes Based on LOCA Separate-Effects Cladding Tests. In: Proceedings of the TopFuel2018 conference.

Pastore, G., Williamson, R.L., Gardner, R.J., Novascone, S.R., Tompkins, J.B., Gamble, K.A., Hales, J.D., 2021b. Analysis of fuel rod behavior during loss-of-coolant accidents using the BISON code: Cladding modeling developments and simulation of separate-effects experiments. J. Nucl. Mater. 543, 152537. https://doi.org/10.1016/J.JNUCMAT.2020.152537.

Perez-Feró, E., Gyori, C., Matus, L., Vasáros, L., Hózer, Z., Windberg, P., Maróti, L., Horváth, M., Nagy, I., Pintér-Csordás, A., Novotny, T., 2010. Experimental database of E110 claddings exposed to accident conditions. J. Nucl. Mater. 397, 48–54. https://doi.org/10.1016/J.JNUCMAT.2009.12.005.

Pizzocri, D., Barani, T., Luzzi, L., 2020. SCIANTIX: A new open source multi-scale code for fission gas behaviour modelling designed for nuclear fuel performance codes. J. Nucl. Mater. 532, 152042 https://doi.org/10.1016/J.JNUCMAT.2020.152042.

Scolaro, A., Clifford, I., Fiorina, C., Pautz, A., 2020. The OFFBEAT multi-dimensional fuel behavior solver. Nucl. Eng. Des. 358, 110416 https://doi.org/10.1016/J.NUCENGDES.2019.110416.

Scolaro, A., Fiorina, C., Clifford, I., Brunetto, E., Pautz, A., 2022. Pre-Release Validation Database for the Multi-Dimensional Fuel Performance Code OFFBEAT, in: International Conference on Physics of Reactors (PHYSOR). pp. 2914–2923. https://doi.org/doi.org/10.13182/PHYSOR22-37789.

Scolaro, A., 2021. Development of a Novel Finite Volume Methodology for Multi-Dimensional Fuel Performance Applications (PhD Thesis). École Polytechnique Fédérale de Lausanne. https://doi.org/10.5075/EPFL-THESIS-8822.

Spencer, B.W., Williamson, R.L., Stafford, D.S., Novascone, S.R., Hales, J.D., Pastore, G., 2016. 3D modeling of missing pellet surface defects in BWR fuel. Nucl. Eng. Des. 307, 155–171. https://doi.org/10.1016/J.NUCENGDES.2016.07.008.

Van Uffelen, P., Hales, J., Li, W., Rossiter, G., Williamson, R., 2019. A review of fuel performance modelling. J. Nucl. Mater. 516, 373–412.

Vlassopoulos, E., Nasyrow, R., Papaioannou, D., Gretter, R., Fongaro, L., Somers, J., Rondinella, V., Caruso, S., Grünberg, P., Helfenstein, J., Schwizer, P., Pautz, A., 2018. Response of irradiated nuclear fuel rods to quasi-static and dynamic loads. Kerntechnik 83, 507–512. https://doi.org/10.3139/124.110948/MACHINEREADABLECITATION/BIBTEX.

Wanninger, A., Seidl, M., Macián-Juan, R., 2018. Mechanical analysis of the bow deformation of a row of fuel assemblies in a PWR core. Nucl. Eng. Technol. 50, 297–305. https://doi.org/10.1016/J.NET.2017.12.009.

Williamson, R.L., Hales, J.D., Novascone, S.R., Tonks, M.R., Gaston, D.R., Permann, C.J., Andrs, D., Martineau, R.C., 2012. Multidimensional multiphysics simulation of nuclear fuel behavior. J. Nucl. Mater. 423, 149–163. https://doi.org/10.1016/J.JNUCMAT.2012.01.012.

Williamson, R.L., Pastore, G., Novascone, S.R., Spencer, B.W., Hales, J.D., 2016. Modelling of LOCA Tests with the BISON Fuel Performance Code. Enlarged Halden Programme Group Meeting.

Appendix B: “A damage model to describe fuel fragmentation and predict fission gas release during Reactivity Initiated Accident”

A damage model to describe fuel fragmentation and predict fission gas release during Reactivity Initiated Accident

Matthieu Reymond[1,2], Jerome Sercombe[2], Alessandro Scolaro[1]
[1] Ecole Fédérale Polytechnique de Lausanne, Switzerland
[2] CEA, DES, IRESNE, DEC, Cadarache, F-13108 Saint-Paul-Lez-Durance, France

ABSTRACT
In this paper, we propose the use of a damage model to describe the mechanical behaviour of nuclear fuel (UO_2) during a Reactivity Initiated Accident. It describes cracking and crushing of the material depending on the loading mode (tension or compression dominated) and on temperature. This model allows one to model fuel's fragmentation and the subsequent Fission Gas Release by coupling the local damage to the release of the intergranular gas inventory. The simulation of the CABRI REP-Na4 and REP-Na5 test pulses showed that the extent of the fragmented zones and the values of the %FGR are in good agreement with the experimental data. The calculations were performed with the fuel performance code OFFBEAT developed at the Ecole Polytechnique Fédérale de Lausanne in Switzerland.

INTRODUCTION
The release of fission gases remains a difficult phenomenon to accurately simulate as pointed out by a recently published synthesis report from NEA (NEA – Working Group on Fuel Satefy, 2022). The main mechanism by which fission gases are released during a fast transient is thought to be grain boundary cracking, as diffusion-based process are too slow to explain the level of release measured after experiments conducted in test reactors. Traditionally, this fuel fragmentation has been attributed to over-pressurisation of the gas bubbles due to the rise of temperature, ultimately leading to grain boundary decohesion (Lemoine, 1997). As a result, in most fuel performance codes, transient fission gas release is often due to grain boundary fragmentation is driven by a stress criterion linked to the bubble internal pressure needed to break the grain boundary (Moal, Georgenthum and Marchand, 2014; Khvostov, 2018; Jernkvist, 2019). Another approach is to directly use a temperature (driving gas bubbles over-pressurisation) threshold triggering the opening of closed porosities at the grain boundaries (Moal, Georgenthum and Marchand, 2014; Pastore *et al.*, 2017). However, grain boundary cracking has been observed after strain-driven compression tests, compression creep tests or bending creep tests on fresh fuel (Byron, 1968; CANON, ROBERTS and BEALS, 1971; Dherbey *et al.*, 2002; Salvo, Sercombe, Helfer, *et al.*, 2015). Moreover, significant grain boundary cracking have been observed on almost the totality of the fuel radius in low burnup (around 30 GWd/tU) fuel rods tested in CABRI such as REP-Na2 (Schmitz and Papin, 1999a). The Fission Gases (FG) inventory for such a burnup is small and cannot explain the extent of the grain boundary fragmentation. Thus, fuel fragmentation cannot be attributed only to gas over-pressurisation.

In this paper, we propose the use of a damage model to simulate grain boundary cracking and fuel fragmentation. The model parametrization is based on the experimental data from Salvo and coworkers (Salvo, Sercombe, Ménard, *et al.*, 2015) that reported significant grain boundary cracking after uniaxial compressive tests performed on fresh fuel at a strain rate of 10^{-1} /s and at temperatures above 1623 K, which are conditions typically encountered during a RIA Transient. Thus, the damage variable of the model is thought to directly represent grain boundary cracking and is used to trigger transient fission gas release when a certain threshold of damage is reached. A threshold of temperature is also considered for the gas release from the restructured zone of the fuel. This methodology is then applied to simulate fuel fragmentation and fission gas release during the CABRI REP-Na4 and REP-Na5 tests.

DAMAGE MODEL FOR UO_2
To model the mechanical behaviour of UO_2 in tension and in compression, the μ-model proposed by Mazars (Mazars, Hamon and Grange, 2015) and classically used for concrete is considered hereafter. It

was previously used for the simulation of out-of-pile high-power laser heating experiments (Reymond *et al.*, 2021) conducted on UO_2 samples leading to fast localized heating of the material similar in terms of kinetics to a RIA. The model was able to accurately predict the location and time of cracking within the sample due to thermal stresses. In this paper, we now propose to extend its use to the simulation of in-pile experiments, such as RIA-tests performed in research reactors.

In this model, the local damage is described by a scalar variable *d* (ranging from 0 to 1) that represents the effective damage of the material and is used to describe the loss of stiffness of the material. Two damage modes are considered for traction and compression, i.e., cracking and crushing, respectively. In our case, crushing damage is directly linked to grain boundary cracking and fragmentation due to compressive loads. Finally, one of the main interests of this model is its ability to model effects such as cracks opening and closure if the loading is reversed.

In the μ-model, the stress-strain relation is given by:

$$\underline{\sigma} = (1-d)\mathbf{C}:\underline{\varepsilon} \tag{1}$$

With $\underline{\sigma}$ the standard Cauchy stress tensor, **C** the elastic tensor and $\underline{\varepsilon}$ the elastic strain tensor. The material is assumed isotropic, and all the properties are defined at the macroscopic scale.

To model damage, the μ-model uses the equivalent strain concept. Cracking and crushing are associated to the following equivalent strains:

$$\varepsilon_t = \frac{I_\varepsilon}{2(1-2\nu)} + \frac{\sqrt{J_\varepsilon}}{2(1+\nu)} \tag{2}$$

$$\varepsilon_c = \frac{I_\varepsilon}{5(1-2\nu)} + \frac{6\sqrt{J_\varepsilon}}{5(1+\nu)} \tag{3}$$

With I_ε, J_ε the first and second invariants of the strain tensor and ν the Poisson's ratio.
Then, two thermodynamic variables, Y_t and Y_c, related to the maximum equivalent strains reached during the loading sequence, are considered:

$$Y_t = Sup[\varepsilon_{0t}, max(\varepsilon_t)] \quad and \quad Y_c = Sup[\varepsilon_{0c}, max(\varepsilon_c)] \tag{4}$$

Before damage onset, Y_t and Y_c are equal to the initial thresholds ε_{0t} and ε_{0c}. The Y driving variable combine Y_t and Y_c, corresponding to tensile and compressive loads, as:

$$Y = rY_t + (1-r)Y_c \tag{5}$$

With r the triaxial factor indicating the nature of the stress. $r = 0$ corresponds to a purely compressive load and $r = 1$ to a purely tensile load.
The effective damage is then computed as:

$$d = 1 - \frac{(1-A)Y_0}{Y} - A\exp\big(-B(Y-Y_0)\big) \tag{6}$$

With Y_0 the corresponding initial threshold for Y:

$$Y_0 = r\varepsilon_{0t} + (1-r)\varepsilon_{0c} \tag{7}$$

The internal variables A and B are computed as:

$$A = A_t\left(2r^2(1-2k) - r(1-4k)\right) + A_c(2r^2 - 3r + 1)$$
$$B = r^{(r^2 r+2)}B_t + \left(1 - r^{(r^2-2r+2)}\right)B_c$$

(8)

When $r = 1$, $A = A_t$ and $B = B_t$ and when $r = 0$, $A = A_c$ and $B = B_c$. As one can see from equations 6 to 9, it is easy to split every variables between their compressive or tensile contribution. Finally, the five parametersA_t, B_t, A_c, B_c and k can be easily identified from strain-stress curves obtained from uniaxial compression and tensile or bending tests. Two strain thresholds activating the damage evolution need also to be defined for tension and compression, i.e., ε_{0t} and ε_{0c} , respectively.

UO_2 exhibits a brittle to ductile transition that is not only dependent on temperature but also on strain rate. Generally speaking, the higher the strain rate, the higher the temperature of transition will be. For example, Salvo et al (Salvo, Sercombe, Helfer, *et al.*, 2015) reported a brittle to ductile transition between 1373 K (1100 °C) and 1623 K (1350 °C) at a strain rate of 10^{-1} /s during uniaxial compression tests. A ductile behaviour was reported for a temperature of 1623 K (1350 °C) while pronounced grain boundary cracking observed by SEM examination was observed at temperatures ≥ 1823 K (1550 °C). At moderate temperature (1373 K), a brittle behaviour with cracks parallel to the stress direction was reported. No grain boundary cracking was observed for strain rates below 10^{-1} /s, indicating that this phenomenon can only happen under high strain rates.

Similar observations have been reported for the tensile domain by Evans and Davidge (Evans and Davidge, 1969) who identified a temperature of transition around 1473 K (1200 °C) from three-point bending tests. Similarly, Canon and coworkers (CANON, ROBERTS and BEALS, 1971) found a temperature of transition of 1473 K from four-point bending tests leading to an ultimate tensile stress of ~120 MPa at a strain rate of 9.2 /h (2.10^{-3} /s). With strain rate usually exceeding 1/s during RIA transients, a brittle behaviour is expected in tension even at high temperatures at which the behaviour would normally be ductile at lower strain rates.

As we aim to model the fragmentation of the fuel -due to grain boundary cracking-, we hereafter propose a parametrization of the μ-model based on the strain-stress curves of Salvo et al (Salvo, Sercombe, Helfer, *et al.*, 2015) obtained during uniaxial compression tests at high strain rates (10^{-1} /s) and high temperatures (1373, 1623, 1823 and 1973 K) representative of RIA loading conditions. This parametrization assumes an elastic behaviour (i.e, no damage onset) for low temperatures and low strain rate and a combination of elasticity and damage at high temperatures and high strain rate. In the model, it corresponds to a threshold of temperature and of equivalent strain rate above which the internal variable Y_c of the model is updated.

To reproduce the behaviour observed by Salvo et al with grain boundary cracking occurring at and above 1823 K (1550 °C) at a minimum strain rate of 10^{-1} /s, the strain rate threshold was set at 10^{-1} /s and the temperature threshold at 1623 K and. This temperature threshold is lower than the temperature at which grain boundary cracking was observed since higher strain rates can be reached in the fuel pellet during a RIA (up to 10 /s). If no significant grain boundary cracking was reported by Salvo et al 1623 K with a strain-rate of 10^{-1} /s, it is expected that the temperature interval in which grain boundary cracking can happen would be larger at high strain rate. Unfortunately, no experimental data at a strain rate superior to 10^{-1} /s are available in the literature to give us a better understanding of the relation between strain rate / temperature and the onset of grain boundary cracking. The equivalent strain rate concept is considered for the threshold on the strain rate and is expressed as:

$$\dot{\varepsilon_{eq}} = \sqrt{\dot{\varepsilon_{xx}^2} + \dot{\varepsilon_{yy}^2} + \dot{\varepsilon_{zz}^2}}$$

(9)

As we assume an elastic behaviour below 1623 K (no update of the internal variables relative to the compressive load) and a quasi-perfect plastic behaviour at or above 1623 K, the A_c parameter is set to 0. Consequently, The B_c parameter can also be set to 0 as it has no impact on damage evolution if A_c is set to 0. Thus, the only parameter that needs to be defined is ε_{0c}, corresponding to the strain at which damage is activated. Salvo's experiments clearly led to a stress plateau which is thought to correspond to the flow stress. Thus, ε_{0c} decreases on the 1623 K-2500 K interval to reproduce the decrease of stress with increasing temperatures, the stress calculated at the ε_{0c} strain being the asymptotic one when $A_c = 0$.

The tensile behaviour is assumed to remain brittle whatever the temperature reached and is characterized by a constant ultimate tensile stress of 140 MPa. Finally, the asymptotic shear stress has been assumed null, leading to $k = 1$. The resulting parameters expressions of the μ-model are given in Table 1.

At	3.5
Bt	1750
ε_{0t}	0.000013
k	1
Ac	0
Bc	0
ε_{0c}	$-3.0226 \times 10^{-10} \times T^2 - 1.8109 \times 10^{-6} \times T + 0.0029$ If $\varepsilon_{0c} < 0.0002 : \varepsilon_{0c} = 0.0002$

Table 1: Parameters of the μ-model for the simulation of grain boundary cracking and tensile cracking. In compression, no values for the parameters are prescribed below 1673 K as damage onset cannot occurs.

Figure 1 (left graph) presents the stress-strain curves obtained by imposing a uniaxial strain on a single cell. As can be seen, in compression, the behaviour below 1623 K is elastic with no damage onset. At temperatures equal or above 1673 K, the behaviour is characterized by a stress peak reached at less than 1% of axial strain followed by a plateau. The stress peak decreases with temperature increase. The tensile behaviour is described by a single curve since no temperature dependency is assumed. The maximum stress reaches ~140 MPa and is followed by a fast decrease of the stress towards a 0 value.

The corresponding damage-strain curves are given in Figure 1 (right graph). The most important aspect of this parametrization is the significant damage obtained in compression even at low strain level (less than 0.5 %), which is consistent with the pronounced grain boundary cracking reported by Salvo et al for the samples tested at high temperatures. As one can see, the proposed parametrization results in an increase in damage with temperature for a given strain level, corresponding to the decrease with temperature of the flow stress observed by Salvo and co-workers.

Fission Gas Release coupling to grain boundary cracking

We relate the fission gas release to grain boundary cracking which is represented in the model by the local damage caused by compressive stresses d_c.

This coupling is based on the following assumptions:

- Grain boundary cracking is associated to the crushing damage d_c. When a threshold of d_c is reached in a given cell, the local inter-granular gas inventory is released from the fuel.
- In case of high burnup fuel, characterised by a fine grain structure and a high fraction of the gas inventory at the grain boundaries, a threshold of temperature is considered. This so-called High Burnup Structure (HBS) forms during the nominal irradiation at the periphery of the pellet. If the temperature threshold is reached, the total gas inventory (intergranular and intragranular) is released. This is consistent with annealing tests which showed FGR from the HBS for temperatures as low as 900 K (Hiernaut *et al.*, 2008). In the following simulations, this threshold was set at 1000 K.

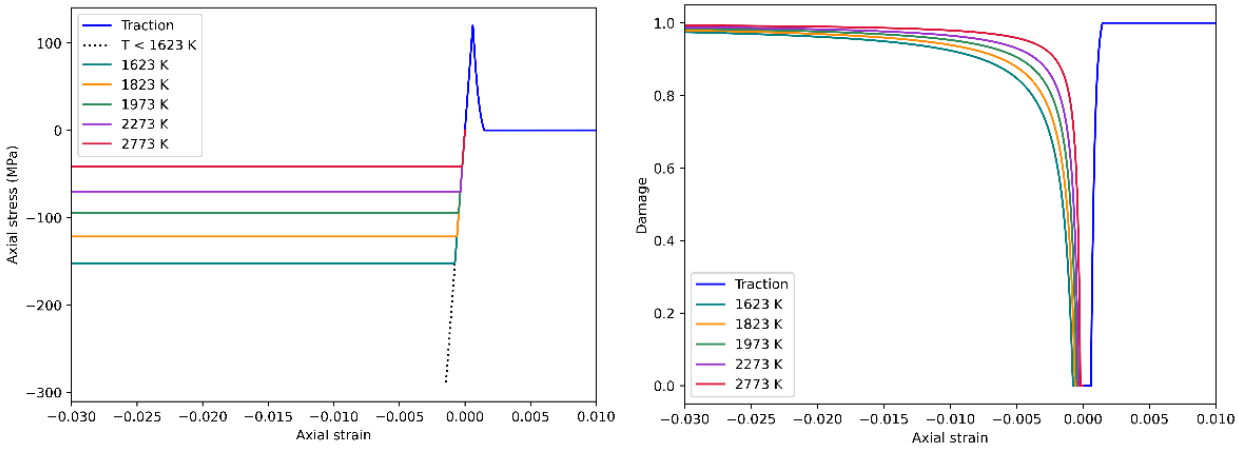

Figure 1: Left: Stress-strain curves at constant temperatures during uniaxial tensile or compressive loading. Right: Corresponding damage-strain curves.

The OFFBEAT fuel performance code

OFFBEAT (Scolaro *et al.*, 2020) is an open-source fuel performance code based on the OpenFOAM C++ library developed at the EPFL and PSI in Switzerland. Until recently, main developments efforts were aimed at modelling fuel behaviour during base irradiation conditions. OFFBEAT has recently been enhanced for RIA simulations on LWR fuel rods. This includes for example the implementation of a specific behaviour law for the clad mechanical behaviour (Le Saux *et al.*, 2008), in addition to the fuel mechanical model presented in this paper for transient fission gas release. We believe all relevant models for RIA simulations on irradiated fuel rods are now available in OFFBEAT. The μ-model and its parametrization have been implemented in OFFBEAT as well as the handling of the FGR based on the local damage of the fuel during a RIA transient. One important feature of OFFBEAT is its ability to perform the base irradiation prior to transient simulations. Continuity between the two simulations is ensured since the code will use the state calculated at the end of the base irradiation to initialize the transient calculation. As this study is focused on the fuel fragmentation during the transient, the simulations presented hereafter were performed on the axial slice located at Peak Power Node (PPN). This choice also reduce computational time

TEST CASES

The CABRI REP-Na program (Papin *et al.*, 2007), carried out between 1993 and 2000, submitted a total of 12 rodlets to simulated RIA transients in the CABRI experimental reactor (France). In this paper, we consider the REP-Na 4 and REP-Na 5 tests as to validate our model and the methodology to estimate the FGR. A comparison between these two tests is of particular interest since the two rodlets had the same father rod (identical burn-up and FG inventory) and were tested with equivalent deposited energy (397 J/g and 430 J/g for REP-Na 4 and 5, respectively), but with different pulse-widths (76.4 ms and 8.8 ms for REP-Na4 and 5, respectively).

This difference led to a noticeable difference in the measured FGR (8.3% for REP-Na4 and 15.1% for REP-Na5), and the post-mortem examination of the rodlets showed that significant fragmentation occurred at the periphery of the fuel for REP-Na 5 but not for REP-Na 4. Thus, these two cases are ideal to test the simulation of fuel fragmentation with the proposed parametrization of the μ-model coupled to FGR. The main characteristics of the tests are summarized in Table 2.

	REP-Na4	REP-Na5
Maximum Burnup (GWd/t)	62.0	64.0
Cladding type	Std Zy-4	Std Zy-4

Energy deposit (J/g)	397	430
Pulse Width (ms)	76.4	8.8
Peak fuel enthalpy (J/g)	364	451
Maximum mean hoop strain (%)	0.4	1.1
Fission gas release (%)	8.30	15.1
Grain boundary cracking	Not visible	Outer periphery

Table 2: Main characteristics of the REP-Na 4 and REP-Na5 test pulses. From (Papin et al.*, 2007).*

BASE IRRADIATION SIMULATION

During base irradiation, the coupling of OFFBEAT with the 0D gas model SCIANTIX (Pizzocri, Barani and Luzzi, 2020) was activated and gas evolution (gas production, diffusion, bubbles growth and coalescence, etc.) and repartition (intergranular, intragranular or released) were calculated in each cell at each time-step. The fuel pellet was discretized with 55 radial elements with a refinement at its periphery to well capture the HBS formation. The cladding was discretized with 15 radial elements.

A single base irradiation simulation considering one axial slice at Peak Power Node was performed for both test cases as the rodlets for REP-Na 4 and REP-Na 5 were refabricated from the same father rod. Even though they were not refabricated from the same level of the father rod, we do not expect significant differences in the fission gas inventory at the end of the base irradiation. The calculated gas inventory and the radial profiles of the total, intragranular, intergranular and released gas contents at the end of the base irradiation are given Figure 2. They are typical of an UO_2 fuel rod irradiated to 60 GWd/tU with a majority of gases located in the grain boundaries at the periphery of the pellet due to the fine grain structure of the High-Burnup Structure.

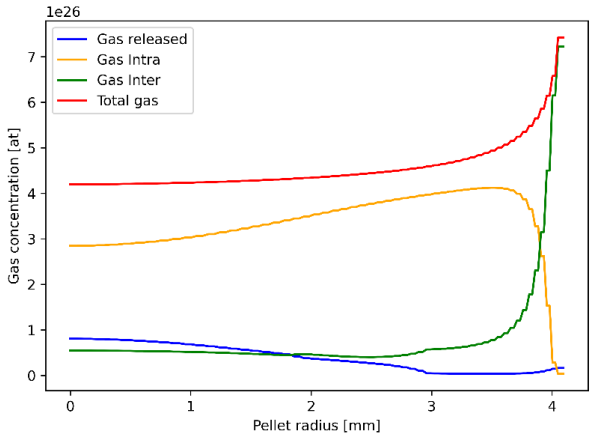

Figure 2: Gas concentration (at) as a function of pellet radius calculated with SCIANTIX at the end of the base irradiation.

RIA TRANSIENT SIMULATIONS

1.5D RIA transient simulations were performed with OFFBEAT for REP-Na 4 and REP-Na 5. The simulations were carried out on a single axial slice located at Peak Power Node. The following modelling hypotheses were considered:

- The parametrization of the μ-model proposed above was used to model the fuel thermo-mechanical behaviour.
- The clad mechanical behaviour is described by the viscoplastic model of Le Saux (Le Saux *et al.*, 2008), established on a large database of tests performed on fresh and irradiated clad samples at temperatures and strain rates typically encountered in RIA conditions.
- The REP-Na tests were performed in a flowing liquid sodium coolant. As OFFBEAT does not have a separate coolant channel model, the clad external temperature evolution was calculated with the ALCYONE fuel code developed by the CEA, EdF and FRAMATOME in the PLEIADES platform (Sercombe et al., 2010)(Guénot-Delahaie et al., 2018) and used as an input in OFFBEAT.

- During these transient simulations, the coupling with SCIANTIX was deactivated as it was not expected that the thermal diffusion of fission gas atoms would have a significant impact during a RIA. Instead, the fission gas release during the transient is handled in a simplified manner by a dedicated module. First, the gas released during the base irradiation is subtracted from the total gas inventory and is reinitialised at 0 at the beginning of the RIA simulation. In the RIA simulations, cells were considered as restructured (i.e., mainly consisting of HBS) if the local burnup was > 80 000 MWd/kgU. This criterion is consistent with the reported thickness of the restructured rim region in the father rod of the REP-Na4 and 5 samples (~200 um) (Schmitz and Papin, 1999b).

Simplified power profiles

As the REP-Na irradiation histories are not publicly available, simplified power pulses were used for the RIA simulations. They are based on the following Gaussian function:

$$f(t) = \frac{1}{\sigma\sqrt{2\pi}} exp\left(-\frac{1}{2}\frac{(t-t_m)^2}{\sigma^2}\right) \quad (10)$$

Where t_m is the time of peak power. The σ value if dependant on the Full Width Half Maximum (FWHM) of the pulse. The resulting power evolutions as a function of time are given in

Inversely, for REP-Na5, significant grain boundary cracking was obtained at the periphery of the pellet on roughly one third of its radius. Figure 5 (left) shows the evolution of the crushing damage, of which the quasi-totality occurred at the end of the pulse. The red colour in the pellet mesh indicates the extent of the area that contributes to fission gas release for a threshold of crushing damage of 0.75 or 0.87. (top).

RESULTS

The radial average peak fuel enthalpies calculated with OFFBEAT and the simplified power pulses reach 375 J/g and 461 J/g for REP-Na 4 and REP-Na 5, respectively. They are consistent with the reported values of 364 J/g and 451 J/g (Papin *et al.*, 2007).

The radial temperature profiles calculated at different times are shown in Figure 3. One stricking difference between the pulse simulations is the peak of temperature induced near the pellet periphery by the fast transient of REP-Na 5 while the temperature profiles of REP-Na 4 are quasi-flat, in accordance with the slow kinetic of the power transient. The maximal temperature reached at the center of the pellet are 1510 and 1678 K for REP-Na4 and REP-Na5, respectively, which is consistent with the deposited energies (430 J/g for REP-Na 5 vs 397 J/g for REP-Na 4).

Evolution of microcracking and resulting fission gas release

The evolution of the local crushing damage, d_c, that is directly linked to grain decohesion is of particular interest as it directly represents the fragmentation of the fuel contributing to FGR. For REP-Na4, a small peak of crushing damage is visible in the area where the thresholds of temperature and strain rate were reached, as one can see on Figure 4 (left). It is however interesting to note that these calculations were made at Peak Power Node, at which the conditions were the most likely to lead to fuel fragmentation. Two damage thresholds were considered to quantify the importance and potential contribution of this damaged zone to the fission gas release: 0.87, at which no fission gas release induced by grain boundary cracking is obtained in REP-Na4 and 0.75, at which the peak of damage visible on Figure 4 (left) contributes to the FGR. The resulting fission gas release as a function of time is plotted in Figure 4 (right). When considering a threshold of 0.87, only the HBS contributes to the calculated FGR and its value is close to the experimental one (9% predicted by OFFBEAT vs the measured 8.1%). When considering a threshold of 0.75, the damaged region also participates to the FGR. The resulting value of 10.7% is nevertheless still consistent

with the experimental one, considering also the probable overprediction due to the choice of PPN for the entire rod, and the typical uncertainties in the measurement of the released volume.

Inversely, for REP-Na5, significant grain boundary cracking was obtained at the periphery of the pellet on roughly one third of its radius. Figure 5 (left) shows the evolution of the crushing damage, of

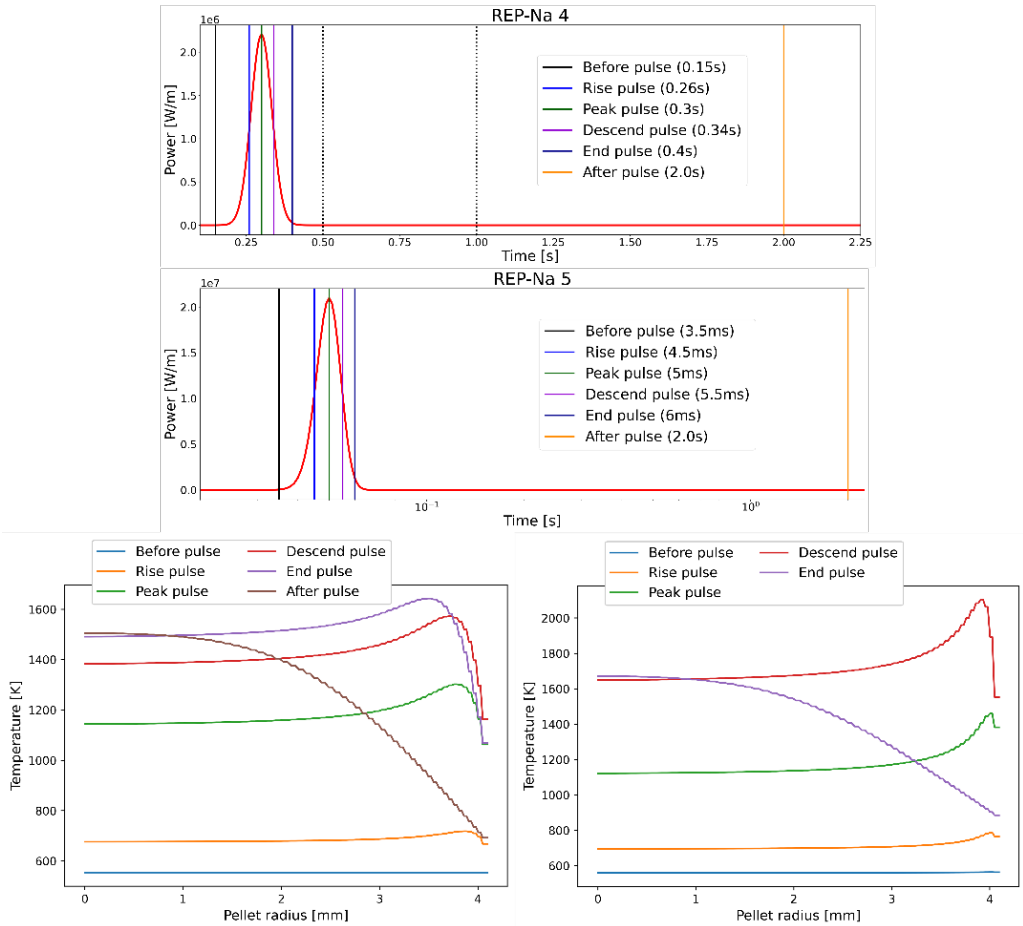

which the quasi-totality occurred at the end of the pulse. The red colour in the pellet mesh indicates the extent of the area that contributes to fission gas release for a threshold of crushing damage of 0.75 or 0.87.

Figure 3: Top: Timeline of the power histories of REP-Na4 and REP-Na5 with the chosen time of plotting for each. Bottom: Radial temperature profiles for REP-Na4 (left) and REP-Na5 (right)

The resulting fission gas release is plotted Figure 5 (right). As for REP-Na4, almost all of the release took place during the power pulse. For a threshold of 0.87, the calculated FGR of 15.2% is in excellent agreement with the measurement of 15.1%. For a threshold of 0.75, the calculated value of 20.8% is still consistent with the measured value. Moreover, the discrepancy between the two pulses is consistent whatever the used damage threshold. It is again worth noting that the simulations were carried at PPN and it is possible that carrying out the same simulation with the same threshold on the whole fuel rodlet would lead to a smaller %FGR as it would be averaged on the whole length of the rod.

CONCLUSION

In this article, we introduced a damage model (the so-called μ-model) coupled to a fission gas model (SCIANTIX) in the OFFBEAT fuel performance code to represent grain boundary cracking and FGR during a RIA transient on UO_2 pellets with. These is models were used to simulate two RIA transients performed at the CABRI facility, i.e., REP-Na4 and REP-Na5.

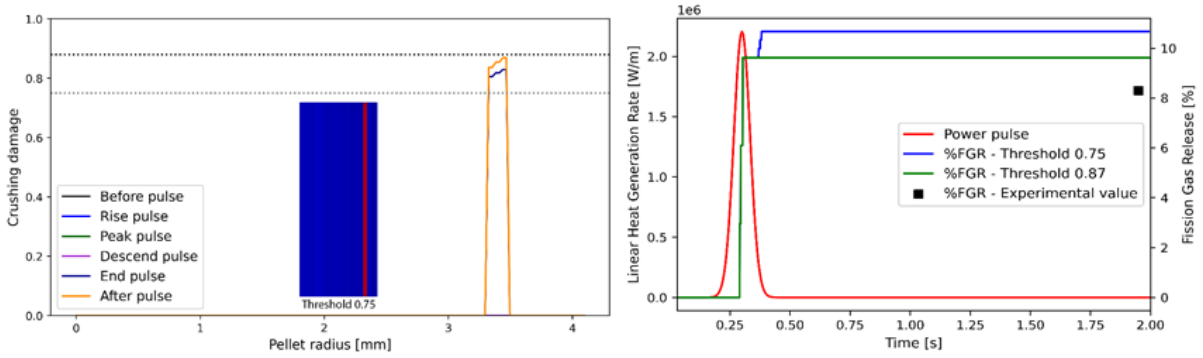

Figure 4: Left: Radial profile of the crushing damage for REP-Na4. The red color in the pellet mesh indicates the extent of the area that contributes to FGR (i.e., that is considered as fragmented) for a threshold of crushing damage of 0.75. Right: Fission gas release as a function of time for REP-Na4. The power pulse is given as a reference.

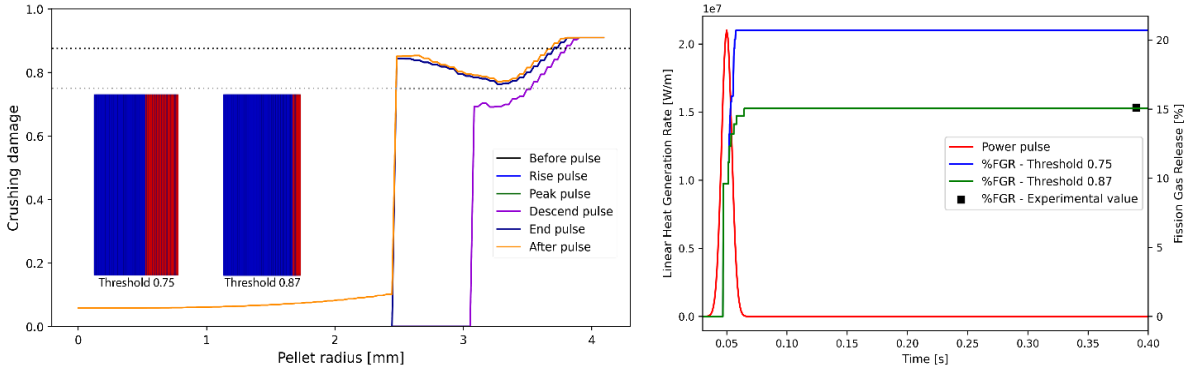

Figure 5: Left: Crushing damage evolution during REP-Na. The black dotted line refers to a damage threshold of 0.85 and the grey dotted line to 0.75. The red color in the pellet meshes indicates the extent of the area that contributes to FGR (i.e., that is considered as fragmented) for the two different thresholds of crushing damage. Right: Fission gas release as a function of time for REP-Na5. The power pulse is given as a reference.

Calculation results have shown that using a mechanistic approach based solely on experimental data obtained on fresh UO_2 is pertinent to accurately model: 1) the onset and radial extent of fuel fragmentation and 2) fission gas release by linking the release to the internal variables of the model representing local grain boundary cracking. Of course, the calculated fission gas release during the transient also greatly depends on the gas inventory and its repartition obtained at the end of the base irradiation. In this regard, OFFBEAT is coupled to the 0D gas model SCIANTIX but the use of others gas models could lead to a different inventory and repartition, thus affecting the transient fission gas behaviour.

Future work could aim at improving the model by, for example, expressing the temperature threshold at which crushing damage can occur as a function of the strain-rate. Its application on other REP-Na test cases for further validation is also envisioned.

Finally, these results also outline the new capabilities of OFFBEAT for the simulation of accidental transients on irradiated fuel rods and its ability to perform both base irradiation and transient behaviour analysis on LWR fuel rods.

REFERENCES

Byron, J.F. (1968) 'Yield and flow of polycrystalline uranium dioxide', *Journal of Nuclear Materials*, 27(1), pp. 48–53.

Canon, R.F. *et al* (1971) 'Deformation of UO2 at High Temperatures', *Journal of the American Ceramic Society*, 54(2), pp. 105–112.

Dherbey, F. *et al.* (2002) *Elevated temperature creep of polycrystalline uranium dioxide: from microscopic mechanisms to macroscopic behaviour*, *Acta Materialia*.
Evans, A.G. and Davidge, R.W. (1969) 'The strength and fracture of stoichiometric polycrystalline UO2', *Journal of Nuclear Materials*, 33(3), pp. 249–260.
Guénot-Delahaie, I. *et al.* (2018) 'Simulation of reactivity-initiated accident transients on UO2-M5® fuel rods with ALCYONE V1.4 fuel performance code', *Nuclear Engineering and Technology*, 50(2), pp. 268–279.
Hiernaut, J.P. *et al.* (2008) 'Fission product release and microstructure changes during laboratory annealing of a very high burn-up fuel specimen', *Journal of Nuclear Materials*, 377(2), pp. 313–324.
Jernkvist, L.O. (2019) ' Modelling of fine fragmentation and fission gas release of UO 2 fuel in accident conditions ', *EPJ Nuclear Sciences & Technologies*, 5, p. 11.
Khvostov, G. (2018) 'Models for numerical simulation of burst FGR in fuel rods under the conditions of RIA', *Nuclear Engineering and Design*, 328, pp. 36–57.
Lemoine, F. (1997) 'High burnup fuel behavior related to fission gas effects under reactivity initiated accidents (RIA) conditions', *Journal of Nuclear Materials*, 248, pp. 238–248.
Mazars, J., Hamon, F. and Grange, S. (2015) 'A new 3D damage model for concrete under monotonic, cyclic and dynamic loadings', *Materials and Structures*, 48(11), pp. 3779–3793.
Moal, A., Georgenthum, V. and Marchand, O. (2014) 'SCANAIR: A transient fuel performance code: Part One: General modelling description', *Nuclear Engineering and Design*, 280, pp. 150–171.
NEA - Working Group on Fuel Satefy (2022) *Nuclear Energy Agency (NEA) - State-of-the-art Report on Nuclear Fuel Behaviour Under Reactivity-initiated Accident Conditions (RIA SOAR)*.
Papin, J. *et al.* (2007) 'Summary and interpretation of the CABRI REP-Na program', *Nuclear Technology*, 157(3), pp. 230–250..
Pastore, G. *et al.* (2017) 'Modeling Fission Gas Behaviour with the BISON Fuel Performance Code'.
Pizzocri, D., Barani, T. and Luzzi, L. (2020) 'SCIANTIX: A new open source multi-scale code for fission gas behaviour modelling designed for nuclear fuel performance codes', *Journal of Nuclear Materials*, 532, p. 152042.
Reymond, M. *et al.* (2021) 'Thermo-mechanical simulations of laser heating experiments on UO2', *Journal of Nuclear Materials*, 557.
Salvo, M., Sercombe, J., Helfer, T., *et al.* (2015) 'Experimental characterization and modeling of UO2 grain boundary cracking at high temperatures and high strain rates', *Journal of Nuclear Materials*, 460, pp. 184–199.
Salvo, M., Sercombe, J., Ménard, J.C., *et al.* (2015) 'Experimental characterization and modelling of UO2 behavior at high temperatures and high strain rates', *Journal of Nuclear Materials*, 456, pp. 54–67.
Le Saux, M. *et al.* (2008) 'A model to describe the anisotropic viscoplastic mechanical behavior of fresh and irradiated Zircaloy-4 fuel claddings under RIA loading conditions', *Journal of Nuclear Materials*, 378(1), pp. 60–69.
Schmitz, F. and Papin, J. (1999a) 'High burnup effects on fuel behaviour under accident conditions: the tests CABRI REP-Na', *Journal of Nuclear Materials*, 270(1), pp. 55–64.
Scolaro, A. *et al.* (2020) 'The OFFBEAT multi-dimensional fuel behavior solver', *Nuclear Engineering and Design*, 358.